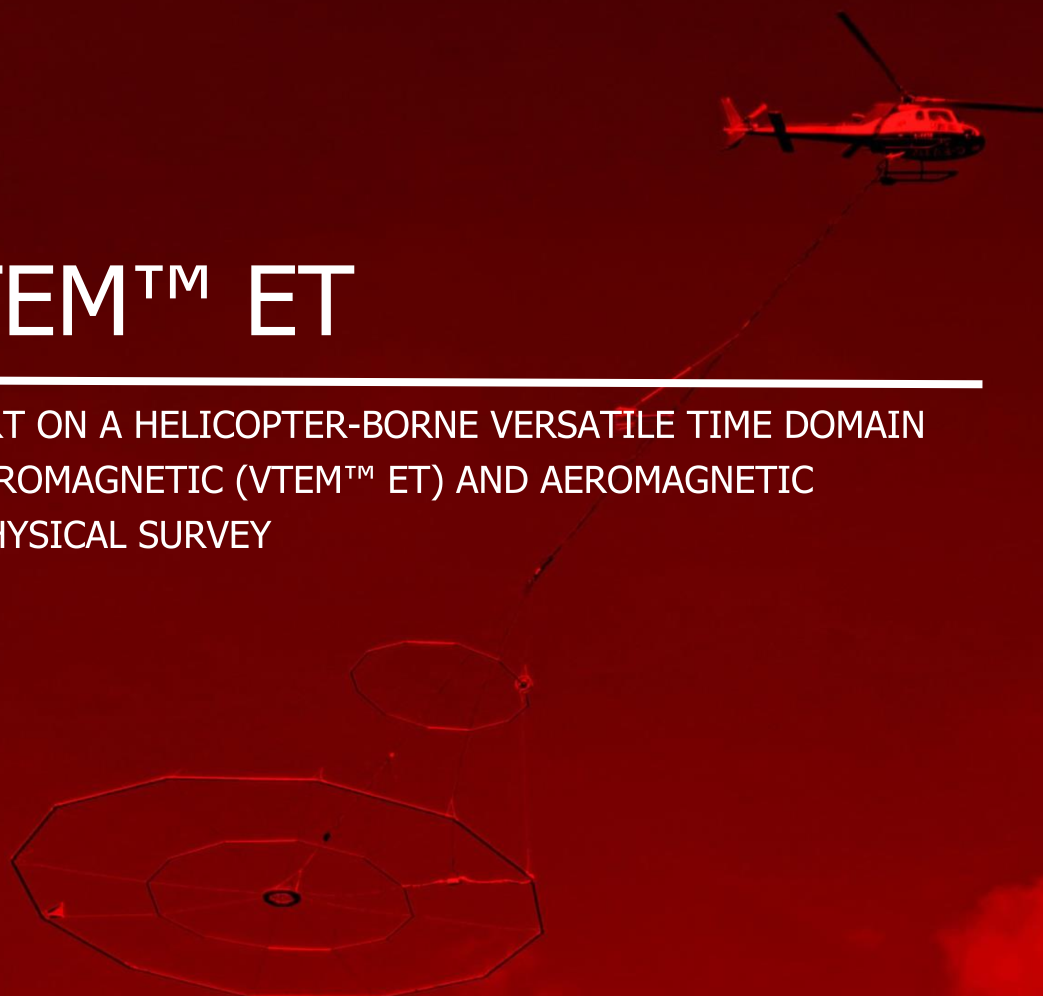

# VTEM™ ET

## REPORT ON A HELICOPTER-BORNE VERSATILE TIME DOMAIN ELECTROMAGNETIC (VTEM™ ET) AND AEROMAGNETIC GEOPHYSICAL SURVEY

| | |
|---|---|
| PROJECT: | SPIRITWOOD-SOUTH AND TOLNA PROJECTS |
| LOCATION: | SPIRITWOOD AND TOLNA, NORTH DAKOTA |
| FOR: | NORTH DAKOTA STATE WATER COMMISSION |
| SURVEY FLOWN: | October 2018 to March 2019 |
| PROJECT: | GL170349B |


Geotech Ltd.
245 Industrial Parkway North
Aurora, ON Canada L4G 4C4

Tel: +1 905 841 5004
Web: www.geotech.ca
Email: info@geotech.ca


GEOTECH
AIRBORNE GEOPHYSICAL SURVEYS

# TABLE OF CONTENTS



# LIST OF FIGURES



# LIST OF TABLES

# APPENDICES

# EXECUTIVE SUMMARY

## SPIRITWOOD-SOUTH AND TOLNA PROJECTS
## JAMESTOWN AND TOLNA REGIONS, NORTH DAKOTA


From October 18, 2018 to March 23, 2019 Geotech Ltd. carried out a helicopter-borne geophysical survey over the Spiritwood-South and Tolna Projects that are situated near Jamestown and Tolna, North Dakota.

Principal geophysical sensors included a versatile time domain electromagnetic (VTEM™ ET) system, and a caesium magnetometer. Ancillary equipment included a GPS navigation system and a radar altimeter. A total of 3084 line-kilometres (3000 km planned) of geophysical data were acquired during the survey.

In-field data quality assurance and preliminary processing were carried out on a daily basis during the acquisition phase. Preliminary and final data processing, including generation of final digital data and map products were undertaken from the office of Geotech Ltd. in Aurora, Ontario.

The processed survey results are presented as the following maps:

- Total Magnetic Intensity (TMI)
- Electromagnetic dB/dt Time Channel Maps
- Calculated Time Constant (Tau) with Calculated Vertical Derivative contours
- Resistivity Depth Images (RDI) sections

The final processed data was inverted to create 1D resistivity models over the entire survey block. The inversions were performed by Geotech and also by Aqua Geo Frameworks (see below). The inversion results were effective at mapping aquifer material in the Spiritwood South and Tolna project areas. These results are presented as:

- Planar resistivity depth slices
- Cross-sectional resistivity models for each flight and tie line
- 3D gridded voxel composed from each 1D inversion model

Digital data includes all electromagnetic and magnetic products, plus ancillary data including the waveform and all inversion modeling products.

The survey report describes the procedures for data acquisition, processing, equipment used, final image presentation and the specifications for the digital data set.

Aqua Geo Frameworks produced a separate report describing their data processing workflow and 1D inversions results. The Aqua Geo Frameworks report and technical products are part of the project deliverables to NDSWC.

# 1. INTRODUCTION

## 1.1 GENERAL CONSIDERATIONS

Geotech Ltd. performed a helicopter-borne geophysical survey over the Spiritwood-South and Tolna Projects situated near Jamestown and Tolna, North Dakota. (Figure 1 & Figure 2).

David Hisz represented North Dakota State Water Commission during the data acquisition and data processing phases of this project.

The geophysical surveys consisted of helicopter borne EM using the versatile time-domain electromagnetic (VTEM™ ET) system with Full-Waveform processing. Measurements consisted of Vertical (Z) component and aeromagnetics using a caesium magnetometer. A total of 3084 line-km of geophysical data were acquired during the survey.

The crew was based out of Jamestown and Devil's Lake, North Dakota for the acquisition phase of the survey. Survey flying was started on October 18th, 2018 and was completed on March 23rd, 2019.

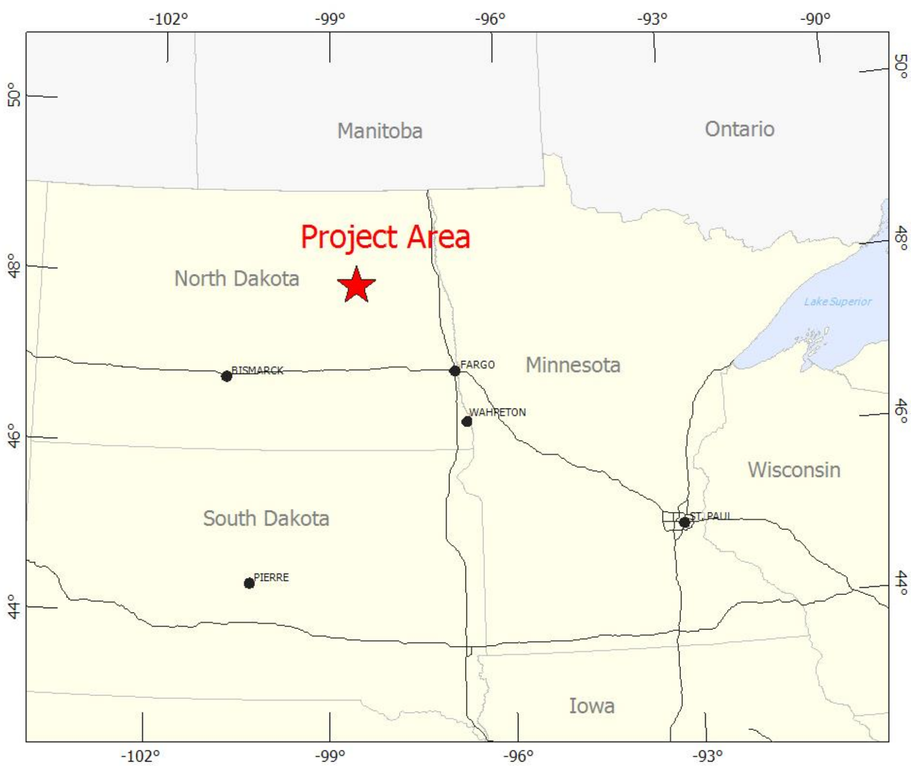


Figure 1: Survey location.

Data quality control and quality assurance, and preliminary data processing were carried out on a daily basis during the acquisition phase of the project. Aqua Geo Frameworks performed additional quality control and laterally constrained 1D inversions (LCI) on the EM data.

Final data processing followed immediately after the end of the survey. Final reporting, data presentation, inversion modeling and archiving were completed from the Aurora office of Geotech Ltd. in June, 2018. Unconstrained 1D layered earth inversions (LEI) were produced by Geotech while Aqua Geo Frameworks performed and spatially constrained inversions (SCI) on the final processed dataset.

## 1.2 SURVEY AND SYSTEM SPECIFICATIONS

The survey areas are located near Jamestown and Tolna, North Dakota (Figure 2).

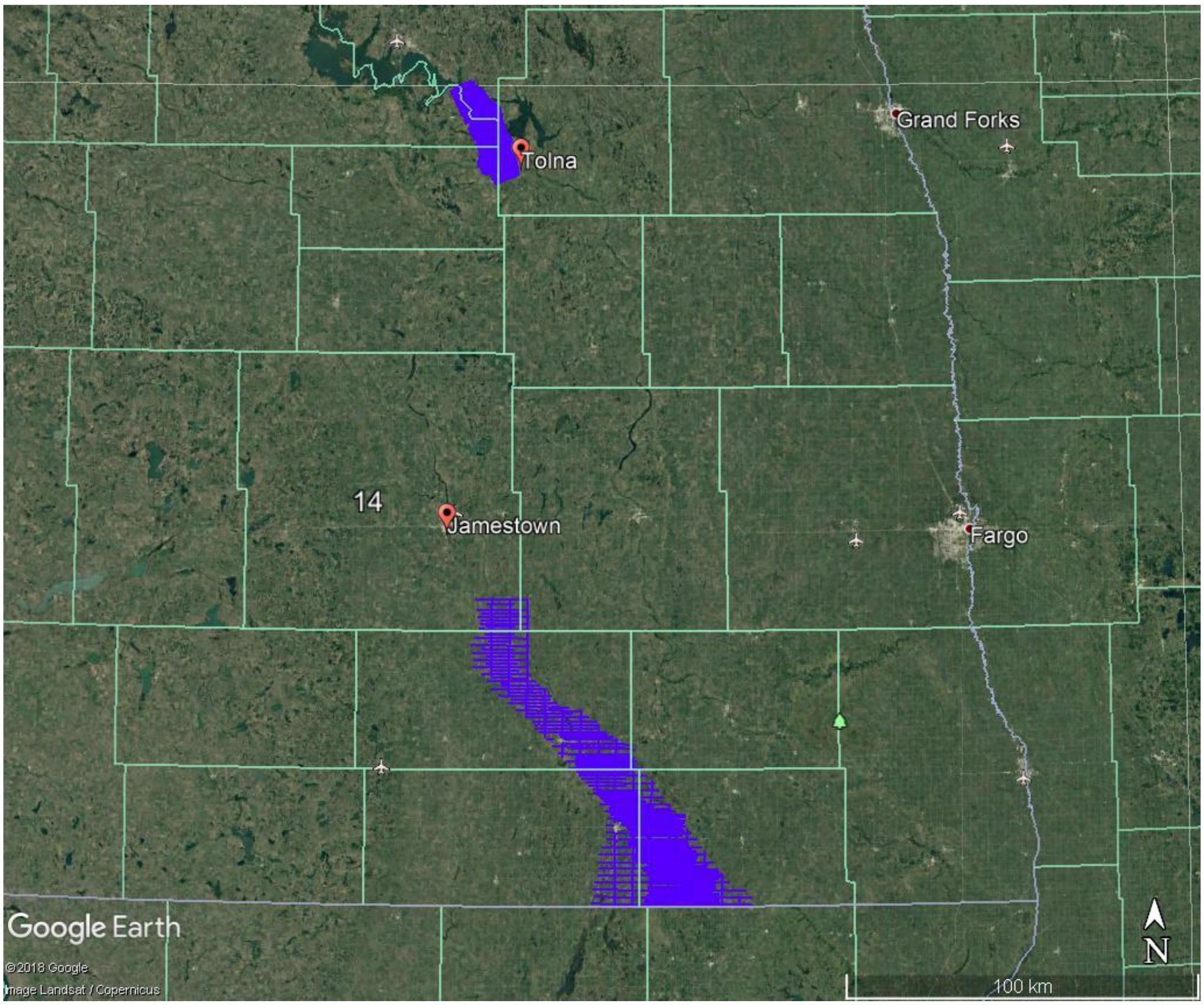


Figure 2: Survey area locations on Google Earth.

The Spiritwood-South area was flown in an east to west (N 90° E azimuth) direction, with multiple line spacings as depicted in Figure 3. Tie lines were flown perpendicular to the traverse lines at a spacing of 5000 metres.

The Tolna area was flown in a northeast to southwest (N 68° E azimuth) direction, with traverse line spacings of 500 metres. For more detailed information on the flight spacing and direction see Table 1.

## 1.3 TOPOGRAPHIC RELIEF AND CULTURAL FEATURES

Topographically, the survey areas exhibit elevations ranging from 352 to 492 metres above mean sea level over a combined area of 2130 square kilometres.

There are various rivers and streams running through the survey areas. There are visible signs of culture such as roads and buildings/habitations throughout the survey blocks.

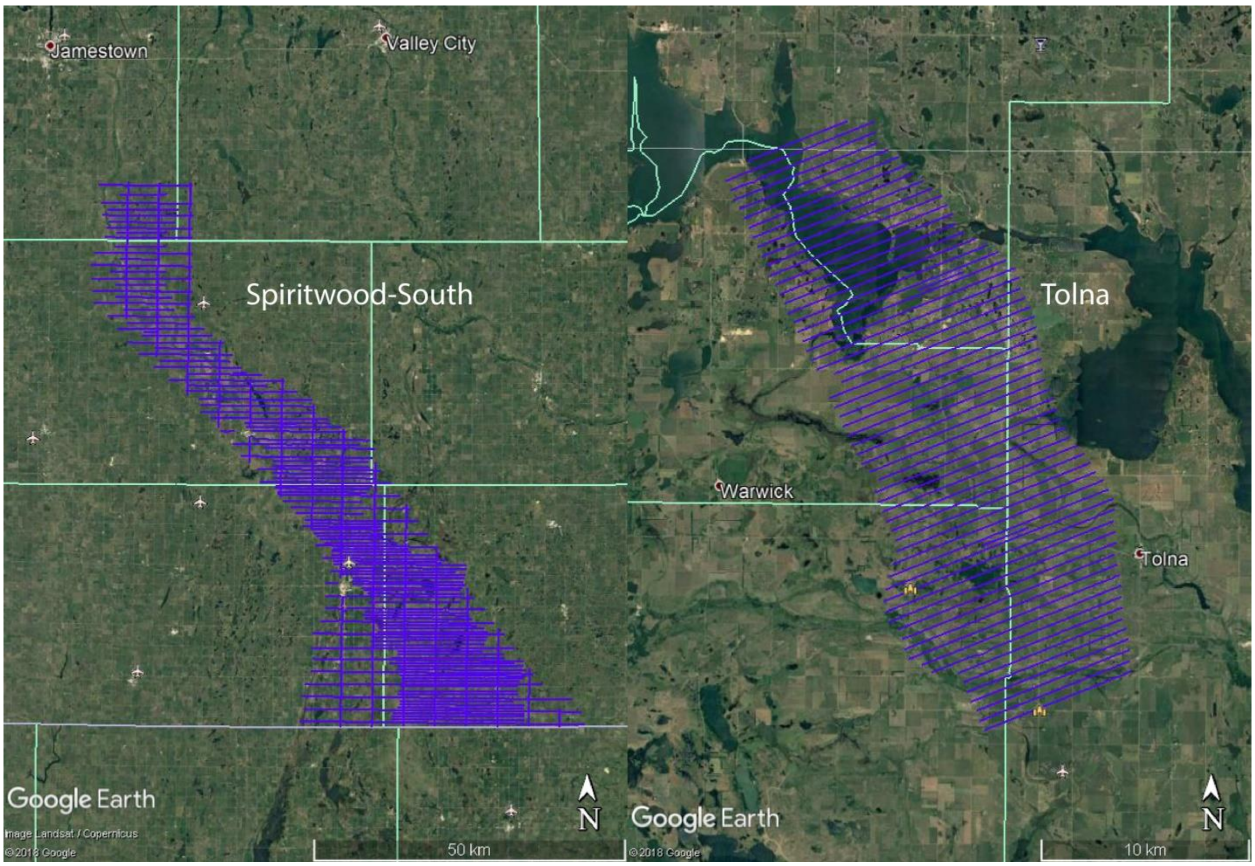


Figure 3: Flight path over a Google Earth Image.

# 2. DATA ACQUISITION

## 2.1 SURVEY AREA

The survey area (see Figure 3 and Appendix A) and general flight specifications are as follows:

Table 1: Survey Specifications

| Survey block | Line spacing (m) | Area ($Km^2$) | Planned[1] Line-km | Actual Line-km | Flight direction | Line numbers |
|---|---|---|---|---|---|---|
| Spiritwood-South | Traverse: 500/1000/2000 | 1848 | 2433 | 2500 | N 90° E / N 270° E | L1000 – L1420 |
| | Tie: 5000 | | | | N 0° E / N 180° E | T5000 – T5140 |
| Tolna | Traverse: 500 | 282 | 567 | 584 | N 68° E / N 148° E | L10000 – L10590 |
| | Tie: n/a | | | | n/a | n/a |
| Total | | 2130 | 3000 | 3084 | | |

Survey area boundaries co-ordinates are provided in Appendix B.

## 2.2 SURVEY OPERATIONS

The crew was based out of Jamestown and Devil's Lake, North Dakota for the acquisition phase of the survey. Survey flying was started on October 18th, 2018 and completed on March 23rd, 2019. The following table shows the timing of the flying.

Table 2: Survey schedule

| Date | Comments |
|---|---|
| 18-Oct-18 | Helicopter and crew arrival in Jamestown, ND. |
| 19-Oct-18 | System assembling. |
| 20-Oct-18 | System assembling. |
| 21-Oct-18 | System testing. |
| 22-Oct-18 | System testing. |
| 23-Oct-18 - 5 Nov-18 | System testing & troubleshooting. |
| 6-Nov-18 | System disassembling and demobilization |
| 7-Dec-18 | System mobilization |
| 8-Dec-18 | System mobilization |
| 9-Dec-18 | Crew arrival in Jamestown, ND. System assembling. |
| 10-Dec-18 | System assembling. |
| 11-Dec-18 | System assembling. |
| 12-Dec-18 | Standby for helicopter arrival. |
| 13-Dec-18 | Standby for helicopter arrival. |
| 14-Dec-18 | Standby for helicopter arrival. |
| 15-Dec-18 | Standby for helicopter arrival. |
| 16-Dec-18 | System installation and testing. |

[1] Note: Actual Line kilometres represent the total line kilometres in the final database. These line-km normally exceed the Planned Line-km, as indicated in the survey NAV files.

| Date | Comments |
| --- | --- |
| 17-Dec-18 | Two production flights completed. ~ 210km flown. |
| 18-Dec-18 | Two production flights completed. ~ 227km flown. |
| 19-Dec-18 | Two production flights completed. ~ 207.5km flown. |
| 20-Dec-18 | One production flight completed. ~ 176.5km flown. |
| 21-Dec-18 | No production flights due to weather conditions. |
| 22-Dec-18 | Crew demobilization for Christmas Break. |
| 5-Jan-19 | Helicopter preparation and crew mobilization to Jamestown, ND. |
| 6-Jan-19 | System and helicopter inspection and preparation. |
| 7-Jan-19 | System set-up and test flight - approved for production. |
| 8-Jan-19 | No production flights due to weather conditions |
| 9-Jan-19 | No production flights due to weather conditions |
| 10-Jan-19 | No production flights due to weather conditions. |
| 11-Jan-19 to 31-Jan-10 | System Troubleshooting |
| 1-Feb-19 | System Testing and 1 production flight. ~ 51km flown. |
| 2-Feb-19 | No production flights due to weather conditions |
| 3-Feb-19 | No production flights due to weather conditions. |
| 4-Feb-19 | No production flights due to weather conditions |
| 5-Feb-19 | One production flight due to weather conditions ~ 27km flown. |
| 6-Feb-19 | No production flights due to poor weather conditions. |
| 7-Feb-19 | No production flights due to poor weather conditions. |
| 8-Feb-19 | No production flights due to poor weather conditions. |
| 9-Feb-19 | No production flights due to poor weather conditions. |
| 10-Feb-19 | No production flights due to poor weather conditions. |
| 11-Feb-19 | One production flight completed. ~62.5km flown. |
| 12-Feb-19 | Crew demobilization and survey paused |
| 5-Mar-19 | Crew mobilization and system testing. |
| 6-Mar-19 | System testing and helicopter maintenance. |
| 7-Mar-19 | Helicopter system installation and test flight. |
| 8-Mar-19 | No production flights due to weather conditions. |
| 9-Mar-19 | No production flights due to weather conditions. |
| 10-Mar-19 | Two production flights completed and South survey area completed. ~ 288.5 km flown. |
| 11-Mar-19 | System mobilization to Devils Lake. |
| 12-Mar-19 | System mobilization to Devils Lake. |
| 13-Mar-19 | No production flights due to strong wind conditions. |
| 14-Mar-19 | No production flights due to strong wind conditions. |
| 15-Mar-19 | One production flight completed. ~ 130.4 km flown. |
| 16-Mar-19 | One production flight completed. ~ 163.2 km flown. |
| 17-Mar-19 | Two production flights completed. ~ 273.1km flown. |
| 18-Mar-19 | System mobilization to Jamestown, ND. |
| 19-Mar-19 | No production flights due to strong wind conditions |
| 20-Mar-19 | Two production flights completed. ~ 330.1 km flown. |
| 21-Mar-19 | Two production flights completed. ~ 258.6 km flown. |
| 22-Mar-19 | Two production flights completed. ~ 341 km flown. |
| 23-Mar-19 | Two production flights completed. ~ 237.4 km flown. Planned flight path for Tolna, Spiritwood and infills are now completed. |

## 2.3 FLIGHT SPECIFICATIONS AND PROCEDURES

During the survey the helicopter was maintained at a mean altitude of 65 metres above the ground with an average survey speed of 80 km/hour. This allowed for an average Transmitter-receiver loop terrain clearance of 36 metres and a magnetic sensor clearance of 56 metres.

The on board operator was responsible for monitoring the system integrity. He also maintained a detailed flight log during the survey, tracking the times of the flight as well as any unusual geophysical or topographic features.

On return of the aircrew to the base camp the survey data was transferred from a compact flash card (PCMCIA) to the data processing computer. The data were then uploaded via ftp to the Geotech office in Aurora for daily quality assurance and quality control by qualified personnel.

## 2.4 AIRCRAFT AND EQUIPMENT

### 2.4.1 SURVEY AIRCRAFT

The survey was flown using a Eurocopter Aerospatiale 350B3 helicopter. The helicopter is owned and operated by Geotech Aviation. Installation of the geophysical and ancillary equipment was carried out by a Geotech Ltd crew.

### 2.4.2 ELECTROMAGNETIC SYSTEM

The electromagnetic system was a Geotech Time Domain EM (VTEM™ ET) full receiver-waveform streamed data recorded system. The "full waveform VTEM system" uses the streamed half-cycle recording of transmitter and receiver waveforms to obtain a complete system response calibration throughout the entire survey flight. VTEM with the Serial number 40 had been used for the survey. The VTEM™ ET transmitter current waveform is shown diagrammatically in Figure 4.

The VTEM™ ET Receiver and transmitter coils were in concentric-coplanar and Z-direction oriented configuration. The Transmitter-receiver loop was towed at a mean distance of 30 metres below the aircraft.

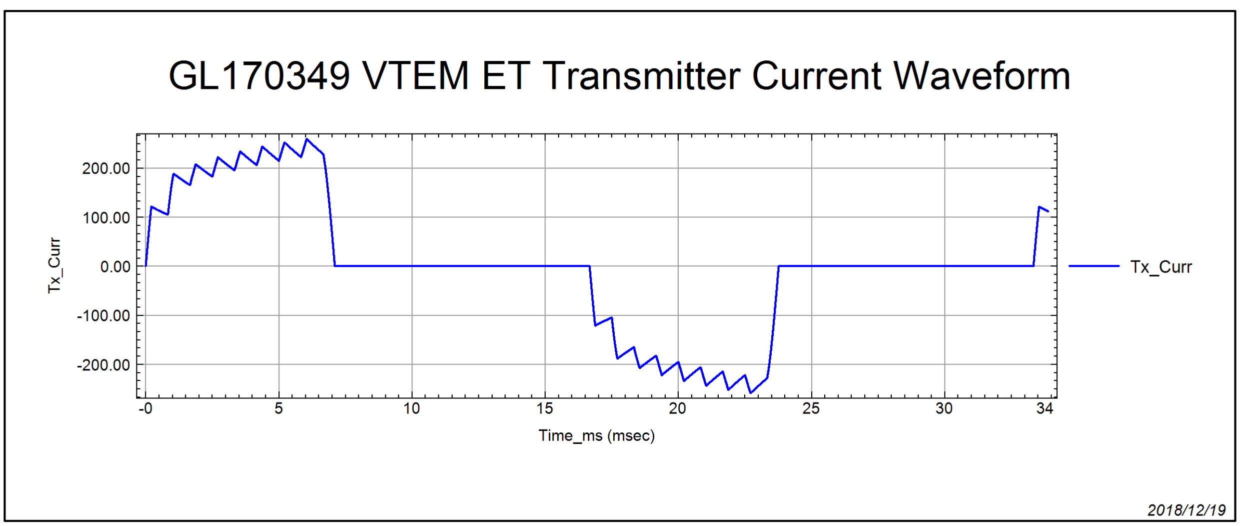


Figure 4: VTEM™ ET Transmitter Current Waveform.

The VTEM™ ET decay sampling scheme is shown in Table 3 below. Fifty four time measurement gates were used for the final data processing in the range from 4.63 to 8254 μsec. Zero time for the off-time sampling scheme is equal to the current pulse width and is defined as the time near the end of the turn-off ramp where the dI/dt waveform falls to 1/2 of its peak value.

Table 3: Off-Time Decay Sampling Scheme

| VTEM ET Decay Sampling Scheme | | | | |
|---|---|---|---|---|
| Index | Start | End | Middle | Width |
| milliseconds | | | | |
| 4 | 0.00405 | 0.00521 | 0.00463 | 0.00116 |
| 5 | 0.00521 | 0.00637 | 0.00579 | 0.00116 |
| 6 | 0.00637 | 0.00752 | 0.00694 | 0.00116 |
| 7 | 0.00752 | 0.00868 | 0.00810 | 0.00116 |
| 8 | 0.00868 | 0.00995 | 0.00926 | 0.00127 |
| 9 | 0.00995 | 0.01146 | 0.01065 | 0.00150 |
| 10 | 0.01146 | 0.01314 | 0.01227 | 0.00168 |
| 11 | 0.01314 | 0.01505 | 0.01400 | 0.00191 |
| 12 | 0.01505 | 0.01730 | 0.01609 | 0.00226 |
| 13 | 0.01730 | 0.01991 | 0.01852 | 0.00260 |
| 14 | 0.01991 | 0.02286 | 0.02130 | 0.00295 |
| 15 | 0.02286 | 0.02622 | 0.02442 | 0.00336 |
| 16 | 0.02622 | 0.03015 | 0.02801 | 0.00394 |
| 17 | 0.03015 | 0.03466 | 0.03229 | 0.00451 |
| 18 | 0.03466 | 0.03981 | 0.03704 | 0.00515 |
| 19 | 0.03981 | 0.04572 | 0.04259 | 0.00590 |
| 20 | 0.04572 | 0.05249 | 0.04884 | 0.00677 |
| 21 | 0.05249 | 0.06030 | 0.05613 | 0.00781 |
| 22 | 0.06030 | 0.06927 | 0.06447 | 0.00897 |
| 23 | 0.06927 | 0.07957 | 0.07407 | 0.01030 |
| 24 | 0.07957 | 0.09138 | 0.08507 | 0.01181 |
| 25 | 0.09138 | 0.10498 | 0.09769 | 0.01360 |
| 26 | 0.10498 | 0.12060 | 0.11227 | 0.01563 |
| 27 | 0.12060 | 0.13854 | 0.12894 | 0.01794 |
| 28 | 0.13854 | 0.15914 | 0.14815 | 0.02060 |
| 29 | 0.15914 | 0.18287 | 0.17014 | 0.02373 |
| 30 | 0.18287 | 0.21007 | 0.19560 | 0.02720 |
| 31 | 0.21007 | 0.24132 | 0.22454 | 0.03125 |
| 32 | 0.24132 | 0.27720 | 0.25810 | 0.03588 |
| 33 | 0.27720 | 0.31829 | 0.29630 | 0.04109 |
| 34 | 0.31829 | 0.36574 | 0.34028 | 0.04745 |
| 35 | 0.36574 | 0.42014 | 0.39120 | 0.05440 |
| 36 | 0.42014 | 0.48264 | 0.44907 | 0.06250 |
| 37 | 0.48264 | 0.55440 | 0.51620 | 0.07176 |
| 38 | 0.55440 | 0.63657 | 0.59259 | 0.08218 |
| 39 | 0.63657 | 0.73148 | 0.68056 | 0.09491 |

| VTEM ET Decay Sampling Scheme | | | | |
|---|---|---|---|---|
| Index | Start | End | Middle | Width |
| milliseconds | | | | |
| 40 | 0.73148 | 0.84028 | 0.78241 | 0.10880 |
| 41 | 0.84028 | 0.96470 | 0.89815 | 0.12442 |
| 42 | 0.96470 | 1.10822 | 1.03125 | 0.14352 |
| 43 | 1.10822 | 1.27315 | 1.18519 | 0.16493 |
| 44 | 1.27315 | 1.46238 | 1.36111 | 0.18924 |
| 45 | 1.46238 | 1.67998 | 1.56366 | 0.21759 |
| 46 | 1.67998 | 1.92998 | 1.79630 | 0.25000 |
| 47 | 1.92998 | 2.21701 | 2.06366 | 0.28704 |
| 48 | 2.21701 | 2.54630 | 2.37037 | 0.32928 |
| 49 | 2.54630 | 2.92477 | 2.72222 | 0.37847 |
| 50 | 2.92477 | 3.35995 | 3.12731 | 0.43519 |
| 51 | 3.35995 | 3.85995 | 3.59259 | 0.50000 |
| 52 | 3.85995 | 4.43403 | 4.12731 | 0.57407 |
| 53 | 4.43403 | 5.09317 | 4.74074 | 0.65914 |
| 54 | 5.09317 | 5.85069 | 5.44560 | 0.75752 |
| 55 | 5.85069 | 6.72049 | 6.25579 | 0.86979 |
| 56 | 6.72049 | 7.71991 | 7.18519 | 0.99942 |
| 57 | 7.71991 | 8.86806 | 8.25463 | 1.14815 |

Z Component: 4- 57 time gates

VTEM™ ET system specifications:

| Transmitter | Receiver |
|---|---|
| • Transmitter loop diameter: 18.82 m<br>• Number of turns: 2<br>• Effective Transmitter loop area: 278 $m^2$<br>• Transmitter base frequency: 30 Hz<br>• Peak current: 259 A<br>• Pulse width: 7.1 ms<br>• Waveform shape: Bi-polar trapezoid<br>• Peak dipole moment: 144,098 nIA<br>• Average transmitter-receiver loop terrain clearance: 36 metres above the ground | • Z-Coil diameter: 1.2 m<br>• Number of turns: 40<br>• Effective coil area: 45.22 $m^2$ |

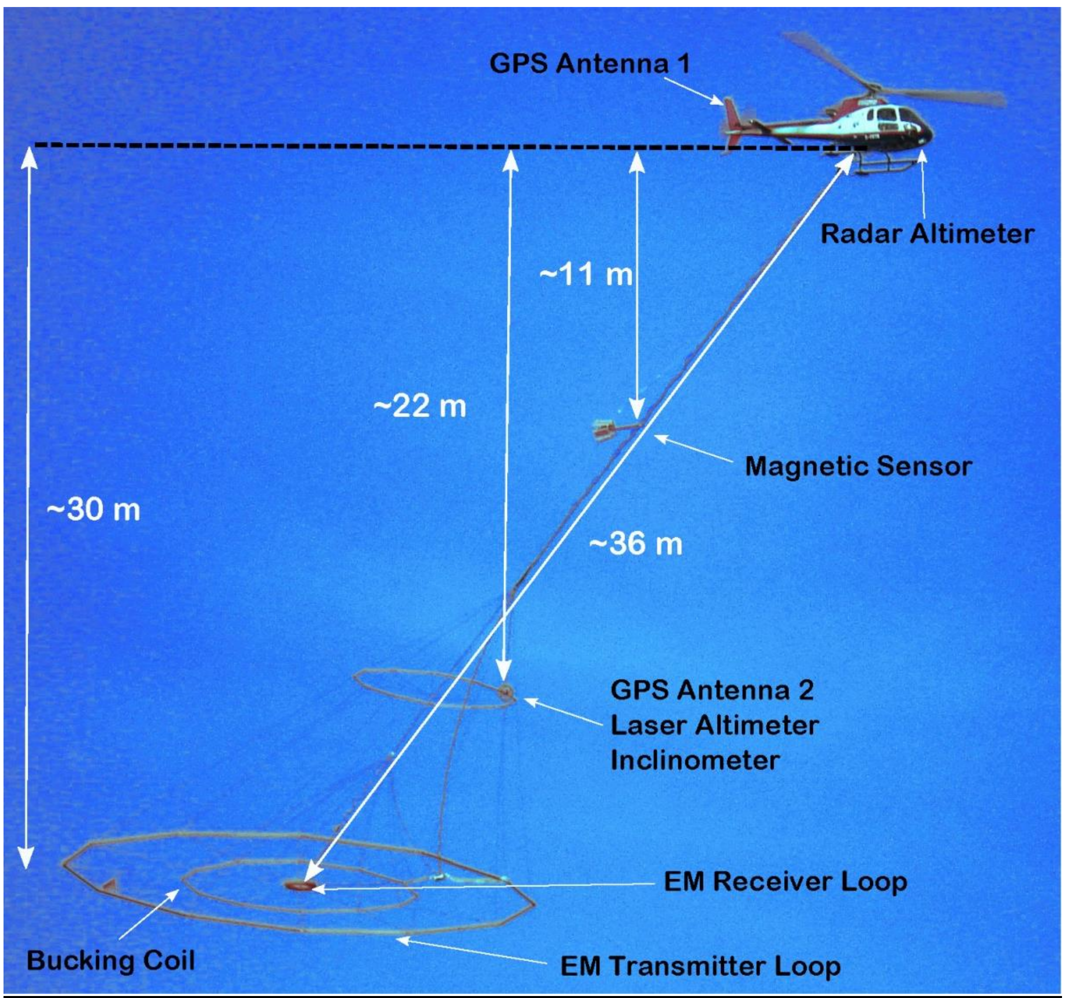


Figure 5: VTEM™ ET System Configuration.

### 2.4.3 FULL WAVEFORM VTEM™ ET SENSOR CALIBRATION

The calibration is performed on the complete VTEM™ ET system installed in and connected to the helicopter, using special calibration equipment. This calibration takes place on the ground at the start of the project prior to surveying.

The procedure takes half-cycle files acquired and calculates a calibration file consisting of a single stacked half-cycle waveform. The purpose of the stacking is to attenuate natural and man-made magnetic signals, leaving only the response to the calibration signal.

This calibration allows the transfer function between the EM receiver and data acquisition system and also the transfer function of the current monitor and data acquisition system to be determined. These calibration results are then used in VTEM full waveform processing.

### 2.4.4 RADAR ALTIMETER

A Terra TRA 3000/TRI 40 radar altimeter was used to record terrain clearance. The antenna was mounted beneath the bubble of the helicopter cockpit (Figure 5).

### 2.4.5 GPS NAVIGATION SYSTEM

The navigation system used was a Geotech PC104 based navigation system utilizing a NovAtel's WAAS (Wide Area Augmentation System) enabled GPS receiver, Geotech navigate software, a full screen display with controls in front of the pilot to direct the flight and a NovAtel GPS antenna mounted on the helicopter tail (Figure 5). As many as 11 GPS and two WAAS satellites may be monitored at any one time. The positional accuracy or circular error probability (CEP) is 1.8 m, with WAAS active, it is 1.0 m. The co-ordinates of the survey area were set-up prior to the survey and the information was fed into the airborne navigation system. The Gyro Inclinometer was not utilized during this survey.

### 2.4.6 DIGITAL ACQUISITION SYSTEM

A Geotech data acquisition system recorded the digital survey data on an internal compact flash card. Data is displayed on an LCD screen as traces to allow the operator to monitor the integrity of the system. The data type and sampling interval as provided in Table 4.

Table 4: Acquisition Sampling Rates

| Data Type | Sampling |
|---|---|
| TDEM | 0.1 sec |
| Magnetometer | 0.1 sec |
| GPS Position | 0.1 sec |
| Radar Altimeter | 0.2 sec |

## 2.5 BASE STATION

A combined magnetometer/GPS base station was utilized on this project. A Geometrics Caesium vapour magnetometer was used as a magnetic sensor with a sensitivity of 0.001 nT. The base station was recording the magnetic field together with the GPS time at 1 Hz on a base station computer.

The base station magnetometer sensor was installed in a secure area away from electric transmission lines and moving ferrous objects such as motor vehicles. The base station data were backed-up to the data processing computer at the end of each survey day.

# 3. PERSONNEL

The following Geotech Ltd. personnel were involved in the project.

FIELD:

| | |
|---|---|
| Project Manager: | Werner Hill (Office) |
| Data QC: | Nick Venter (Office) |
| | Neil Fiset (Office) |
| Crew chief: | Colin Lennox |
| | Paul Taylor |
| | Rafael Coyoli |
| | Adolf Masiyandima |
| | Oscar Gomez |

The survey pilot and the mechanical engineer were employed directly by the helicopter operator – Geotech Aviation.

| | |
|---|---|
| Pilot: | Shanne Kochan |
| | Brent Jewel |
| | Guy Lajoie |
| Mechanical Engineer (AME): | Dylan Pike, |
| | Ian Boychuck |
| | Daniel Buckles |

OFFICE:

| | |
|---|---|
| Preliminary Data Processing: | Nick Venter |
| Final Data Processing: | Zihao Han |
| Data QA/QC: | Kanita Khaled |
| Reporting/Mapping: | Kyle Orlowski |

Processing and Interpretation phases were carried out under the supervision of Kanita Khaled, P.Geo. The customer relations were looked after by Jean Legault, P.Geo.

# 4. DATA PROCESSING AND PRESENTATION

Data compilation and processing were carried out by the application of Geosoft OASIS Montaj and programs proprietary to Geotech Ltd.

## 4.1 FLIGHT PATH

The flight path, recorded by the acquisition program as WGS 84 latitude/longitude, was converted into the WGS84 Datum, UTM Zone 14 North coordinate system in Oasis Montaj.

The flight path was drawn using linear interpolation between x, y positions from the navigation system. Positions are updated every second and expressed as UTM easting's (x) and UTM northing's (y).

## 4.2 ELECTROMAGNETIC DATA

The Full Waveform EM specific data processing operations included:

- Half cycle stacking (performed at time of acquisition);
- System response correction;
- Parasitic and drift removal.

A three stage digital filtering process was used to reject major sferic events and to reduce system noise. Local sferic activity can produce sharp, large amplitude events that cannot be removed by conventional filtering procedures. Smoothing or stacking will reduce their amplitude but leave a broader residual response that can be confused with geological phenomena. To avoid this possibility, a computer algorithm searches out and rejects the major sferic events. VLF interferences were observed in the EM data. The following frequencies were identified and removed: 24.0kHz, 24.8kHz and 25.2kHz.

The signal to noise ratio was further improved by the application of a low pass linear digital filter. This filter has zero phase shift which prevents any lag or peak displacement from occurring, and it suppresses only variations with a wavelength less than about 1 second or 15 metres. This filter is a symmetrical 1 sec linear filter.

The results are presented as stacked profiles of EM voltages for the time gates, in linear - logarithmic scale for the dB/dt responses in the Z component. Calculated Time Constant (TAU) with Calculated Vertical Derivative contours is presented in Appendix C and E. Resistivity Depth Image (RDI) is also presented in Appendix F and G.

VTEM™ receiver coil orientation Z-axis coil is oriented parallel to the transmitter coil axis and both are horizontal to the ground. Generalized modeling results of VTEM data, are shown in Appendix D.

Z component data produce double peak type anomalies for "thin" sub vertical targets and single peak for "thick" targets.

The limits and change-over of "thin-thick" depends on dimensions of a TEM system (Appendix D, Figure D-16).

The early channel decays are examined and compared to any available apriori geologic or geoelectric data or defaulting to standard EM sounding curves. The final step is to set calibration coefficients to earliest time gates assisted by 1D modeling barring any visible AIP effects. Insofar as late time gates no calibration is applied or required.

## 4.3 MAGNETIC DATA

The processing of the magnetic data involved the correction for diurnal variations by using the digitally recorded ground base station magnetic values. The base station magnetometer data was edited and merged into the Geosoft GDB database on a daily basis. The aeromagnetic data was corrected for diurnal variations by subtracting the observed magnetic base station deviations.

Tie line levelling was carried out by adjusting intersection points along traverse lines. A micro-levelling procedure was applied to remove persistent low-amplitude components of flight-line noise remaining in the data.

The corrected magnetic data was interpolated between survey lines using a random point gridding method to yield x-y grid values for a standard grid cell size of 50 metres at the mapping scale. The Minimum Curvature algorithm was used to interpolate values onto a rectangular regular spaced grid.

# 5. 1D INVERSION MODELS

The final processed data was used as the input modeling over the entire block. The algorithm used for the inversion modeling was GALEISBSTDEM2 which is a one dimensional (1D) layered earth deterministic algorithm designed to invert airborne time-domain electromagnetic data. Since the algorithm is 1D, it assumes that the Earth is horizontally stratified and laterally-uniform layer conductivities and thicknesses. For VTEM, the 1D assumption works well in a stratified geology due to the limited lateral sensitivity of the system's measurement outside of its footprint3. Each of these 1D inversion models can be "stitched" together to form visualizations of the layer conductivities along the flight line in 2D and for the entire block in 3D.

The GALEISBSTDEM algorithm has two modeling options: a multi-layer smooth model which solves for the layer's conductivity while the thicknesses remain fixed, or a few-layer blocky model which solves for both the layer's conductivity and thickness. Since the inversion problem for AEM is under-determined, the solution is non-unique and regularization is needed to constrain the model results. The multi-layer smooth model constrains the inversion by fitting only smoothly varying conductivity models with respect to depth which acts as a way to regularize the results. The main constraint for a few-layer blocky model is the number of initial layers in the reference model since this option attempts to resolve a model that reflects the conductivity and thickness of each geological layer. The multi-layer smooth model option works best when there is little prior information about the expected model results due to the smooth nature of the regularization. However, this option is not able to accurately define individual geological layer thicknesses, conductivities, or depths to geological boundaries. To resolve those, the few-layer blocky model option is necessary but requires accurate estimations of the starting models number of layers and conductivity. The blocky model option has the ability to apply probabilistic constraints to each of the conductivity and thickness values in the starting model. These constraints restrict or penalize the inversion algorithm from deviating from the starting model values. Therefore, this additional method of constraining the inversion can be use when there is prior information about the geology, like well logs or boreholes.

For this survey, the inversion process began by using the multi-layer smooth option to model the final processed data. The starting model consisted of 30 layers. Each of these layers started from resistivity of 100 ohm-m. This inversion and each subsequent inversion run inverted every 10th sounding which results in a separation of 25-30 metres for each inverted model. The inversion was able to fit these models within the misfit for each of the soundings not heavily influence by cultural noise. The inversion model results were able to show the general structure of the geology's conductivity profile.

From the 1D inversion results, several products were generated which visualize the resistivity models in different perspectives. The products include: resistivity-depth sections for each survey line; resistivity-depth slices-from surface to the depth of investigation with 10m increments; and 3D gridded resistivity voxels (Figure 6) composed from each of the individual 1D resistivity inversion models that provides a 3D perspective of the resistivity variation across the entire survey block.

---

[2] https://github.com/GeoscienceAustralia/ga-aem

[3] Reid et al. 2006, Airborne electromagnetic footprints in 1D earths: Geophysics, 71, no. 2, pG63-G72.

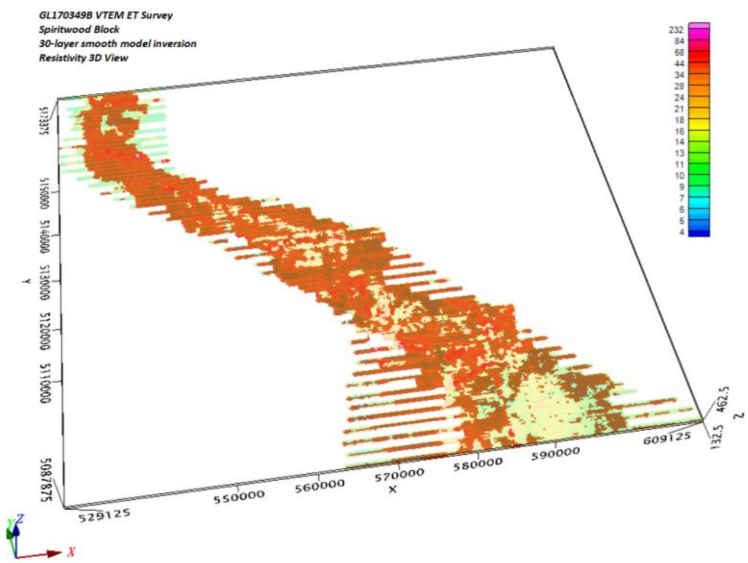


Figure 6 – 3D View of 1D GALEI inversion resistivity voxel for Spiritwood Block (units are in ohm-m).

## 5.1 1D INVERSIONS FOR ISOPACHS

In order to create isopach map products, the procedure involved performing an additional set of 1D inversion of the final VTEM data using the "*few-layer blocky*" option in the GALEI 1D inversion code. A fixed 10-layer model was selected with 9 layers where the inversion solved for the conductivity and thickness plus a basement layer (10). The starting model used is as below, starting with layer 1:

Resistivity (ohm-m) = 10.0, 20.0, 33.3, 11.1, 2.22, 5.90, 20.0, 66.7, 100.0, 100.0

Thickness (metres) = 1.00, 3.00, 5.00, 10.0, 15.0, 30.0, 30.0, 30.0, 30.0

The individual layer thicknesses and resistivities were allowed to vary without constraints. The blocky model results are presented as Isopach layer thickness and resistivity maps (Figure 7). The blocky-layer 1D inversion results are not presented as section plots but have been combined and stored in gdb format and as 3D voxel of the 1D block model resistivity.

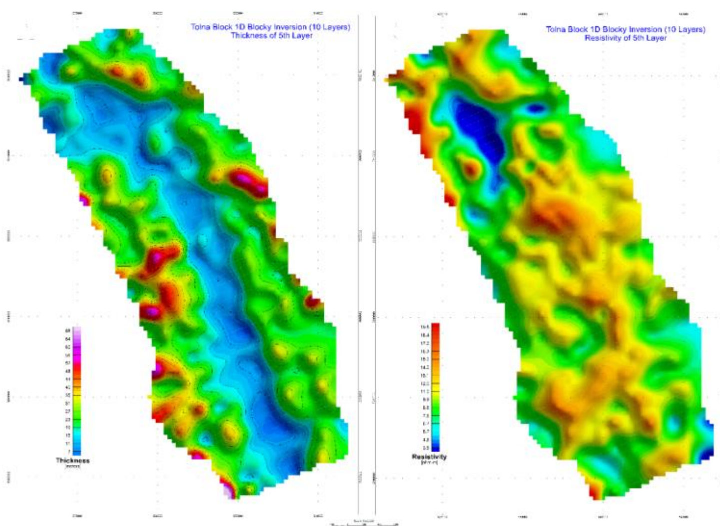


Figure 7 – Isopach layer thickness (left) and resistivity (right) from blocky-model 1D inversion for Tolna.

# 6. DELIVERABLES

## 6.1 SURVEY REPORT

The survey report describes the data acquisition, processing, and final presentation of the survey results. The survey report is provided in two paper copies and digitally in PDF format.

Aqua Geo Frameworks produced an inversion report that accompanies these survey results. Their report[4] focuses on the laterally constrained (LCI) and spatially constrained (SDI) 1D inversion of the VTEM data and their comparisons with borehole results.

## 6.2 MAPS

Final maps were produced at scales of 1:50,000 for Tolna and 1:75,000 for Spiritwood-South for best representation of the survey size and line spacing. The coordinate/projection system used was WGS84 Datum, UTM Zone 14 North. All maps show the flight path trace and topographic data; latitude and longitude are also noted on maps.

- Maps in Geosoft MAP format, as follows:

| | |
|---|---|
| GL170349B_**k_bn_SFz15: | VTEM dB/dt Z Component, Channel 15, Time Gate 0.02442 ms |
| GL170349B_**k_bn_SFz35: | VTEM dB/dt Z Component, Channel 35, Time Gate 0.3912 ms |
| GL170349B_**k_bn_SFz50: | VTEM dB/dt Z Component, Channel 50, Time Gate 3.12731 ms |
| GL170349B_**k_bn_TMI: | Total Magnetic Intensity (TMI) colour image and contours. |
| GL170349B_**k_bn_TauSF: | dB/dt Calculated Time Constant (Tau) with Calculated Vertical Derivative contours |

- Maps are also presented in PDF format.

- The topographic data was derived from North Dakota GIS Hub Data Portal (https://gishubdata.nd.gov/), US Government Open Data (https://www.data.gov/) and Geocommunities (www.geocomm.com)

- A Google Earth file *GL170349B_NDSWC.kmz* showing the flight path of the block is included. Free versions of Google Earth software from: http://earth.google.com/download-earth.html

4 Abraham, J.D., and Asch, T.H., 2019, Final Spatially-Constrained Inversions Report and Data Delivery for the Airborne Electromagnetic Surveys of the Spiritwood South and Tolna Areas, North Dakota for the North Dakota State Water Commission: Technical report by Aqua Geo Frameworks LLC for NDSWC, 69 p.

## 6.3 DIGITAL DATA

Two copies of the data and maps on DVD were prepared to accompany the report. Each DVD contains a digital file of the line data in GDB Geosoft Montaj format as well as the maps in Geosoft Montaj Map and PDF format.

- DVD structure.

Data contains databases, grids and maps, as described below.
Report contains a copy of the report and appendices in PDF format.

Databases in Geosoft GDB format, containing the channels listed in Table 5.

Table 5: Geosoft GDB Data Format

| Channel name | Units | Description |
|---|---|---|
| X: | metres | UTM Easting WGS84 Zone 14 North |
| Y: | metres | UTM Northing WGS84 Zone 14 North |
| Longitude: | Decimal Degrees | WGS 84 Longitude data |
| Latitude: | Decimal Degrees | WGS 84 Latitude data |
| Z: | metres | GPS antenna elevation (above Geoid) |
| Zb: | metres | EM bird elevation (above Geoid) |
| Radar: | metres | helicopter terrain clearance from radar altimeter |
| Radarb: | metres | Calculated EM transmitter-receiver loop terrain clearance from radar altimeter |
| Laser | meters | Laser altimeter height above ground |
| LaserB | meters | Calculated EM transmitter-receiver loop terrain clearance from laser altimeter |
| DEM: | metres | Digital Elevation Model |
| Gtime: | Seconds of the day | GPS time |
| Mag1: | nT | Raw Total Magnetic field data |
| Basemag: | nT | Magnetic diurnal variation data |
| Mag2: | nT | Diurnal corrected Total Magnetic field data |
| Mag3: | nT | Levelled Total Magnetic field data |
| TMI_RES | nT | IGRF removed mag3 |
| CVG: | nT/m | Calculated vertical gradient of TMI |
| SFz[4] | $pV/(A*m^4)$ | Z dB/dt 0.00463 millisecond time channel |
| SFz[5] | $pV/(A*m^4)$ | Z dB/dt 0.00579 millisecond time channel |
| SFz[6] | $pV/(A*m^4)$ | Z dB/dt 0.00694 millisecond time channel |
| SFz[7] | $pV/(A*m^4)$ | Z dB/dt 0.00810 millisecond time channel |
| SFz[8]: | $pV/(A*m^4)$ | Z dB/dt 0.00926 millisecond time channel |
| SFz[9]: | $pV/(A*m^4)$ | Z dB/dt 0.01065 millisecond time channel |
| SFz[10]: | $pV/(A*m^4)$ | Z dB/dt 0.01227 millisecond time channel |
| SFz[11]: | $pV/(A*m^4)$ | Z dB/dt 0.01400 millisecond time channel |
| SFz[12]: | $pV/(A*m^4)$ | Z dB/dt 0.01609 millisecond time channel |
| SFz[13]: | $pV/(A*m^4)$ | Z dB/dt 0.01852 millisecond time channel |
| SFz[14]: | $pV/(A*m^4)$ | Z dB/dt 0.02130 millisecond time channel |
| SFz[15]: | $pV/(A*m^4)$ | Z dB/dt 0.02442 millisecond time channel |
| SFz[16]: | $pV/(A*m^4)$ | Z dB/dt 0.02801 millisecond time channel |
| SFz[17]: | $pV/(A*m^4)$ | Z dB/dt 0.03229 millisecond time channel |

| Channel name | Units | Description |
|---|---|---|
| SFz[18]: | pV/(A*$m^4$) | Z dB/dt 0.03704 millisecond time channel |
| SFz[19]: | pV/(A*$m^4$) | Z dB/dt 0.04259 millisecond time channel |
| SFz[20]: | pV/(A*$m^4$) | Z dB/dt 0.04884 millisecond time channel |
| SFz[21]: | pV/(A*$m^4$) | Z dB/dt 0.05613 millisecond time channel |
| SFz[22]: | pV/(A*$m^4$) | Z dB/dt 0.06447 millisecond time channel |
| SFz[23]: | pV/(A*$m^4$) | Z dB/dt 0.07407 millisecond time channel |
| SFz[24]: | pV/(A*$m^4$) | Z dB/dt 0.08507 millisecond time channel |
| SFz[25]: | pV/(A*$m^4$) | Z dB/dt 0.09769 millisecond time channel |
| SFz[26]: | pV/(A*$m^4$) | Z dB/dt 0.11227 millisecond time channel |
| SFz[27]: | pV/(A*$m^4$) | Z dB/dt 0.12894 millisecond time channel |
| SFz[28]: | pV/(A*$m^4$) | Z dB/dt 0.14815 millisecond time channel |
| SFz[29]: | pV/(A*$m^4$) | Z dB/dt 0.17014 millisecond time channel |
| SFz[30]: | pV/(A*$m^4$) | Z dB/dt 0.19560 millisecond time channel |
| SFz[31]: | pV/(A*$m^4$) | Z dB/dt 0.22454 millisecond time channel |
| SFz[32]: | pV/(A*$m^4$) | Z dB/dt 0.25810 millisecond time channel |
| SFz[33]: | pV/(A*$m^4$) | Z dB/dt 0.29630 millisecond time channel |
| SFz[34]: | pV/(A*$m^4$) | Z dB/dt 0.34028 millisecond time channel |
| SFz[35]: | pV/(A*$m^4$) | Z dB/dt 0.39120 millisecond time channel |
| SFz[36]: | pV/(A*$m^4$) | Z dB/dt 0.44907 millisecond time channel |
| SFz[37]: | pV/(A*$m^4$) | Z dB/dt 0.51620 millisecond time channel |
| SFz[38]: | pV/(A*$m^4$) | Z dB/dt 0.59259 millisecond time channel |
| SFz[39]: | pV/(A*$m^4$) | Z dB/dt 0.68056 millisecond time channel |
| SFz[40]: | pV/(A*$m^4$) | Z dB/dt 0.78241 millisecond time channel |
| SFz[41]: | pV/(A*$m^4$) | Z dB/dt 0.89815 millisecond time channel |
| SFz[42]: | pV/(A*$m^4$) | Z dB/dt 1.03125 millisecond time channel |
| SFz[43]: | pV/(A*$m^4$) | Z dB/dt 1.18519 millisecond time channel |
| SFz[44]: | pV/(A*$m^4$) | Z dB/dt 1.36111 millisecond time channel |
| SFz[45]: | pV/(A*$m^4$) | Z dB/dt 1.56366 millisecond time channel |
| SFz[46]: | pV/(A*$m^4$) | Z dB/dt 1.79630 millisecond time channel |
| SFz[47]: | pV/(A*m4) | Z dB/dt 2.06366 millisecond time channel |
| SFz[48]: | pV/(A*m4) | Z dB/dt 2.37037 millisecond time channel |
| SFz[49]: | pV/(A*m4) | Z dB/dt 2.72222 millisecond time channel |
| SFz[50]: | pV/(A*m4) | Z dB/dt 3.12731 millisecond time channel |
| SFz[51]: | pV/(A*m4) | Z dB/dt 3.59259 millisecond time channel |
| SFz[52]: | pV/(A*m4) | Z dB/dt 4.12731 millisecond time channel |
| SFz[53]: | pV/(A*m4) | Z dB/dt 4.74074 millisecond time channel |
| SFz[54]: | pV/(A*m4) | Z dB/dt 5.44560 millisecond time channel |
| SFz[55]: | pV/(A*m4) | Z dB/dt 6.25579 millisecond time channel |
| SFz[56]: | pV/(A*m4) | Z dB/dt 7.18519 millisecond time channel |
| SFz[57]: | pV/(A*m4) | Z dB/dt 8.25463 millisecond time channel |
| SRawz | pV/(A*$m^4$) | Raw Z dB/dt data for time channels 4 to 57 |
| SFltz | pV/(A*$m^4$) | Filtered Z dB/dt data for time channels 4 to 57 |
| NchanSF | | Latest time channels of TAU calculation |
| TauSF | ms | Time constant dB/dt |
| PLM: | | 60 Hz power line monitor |

dB/dt Z component data is found in array channel format between indexes 8 – 57, as described above.

- Database of the Resistivity Depth Images in Geosoft GDB format, containing the following channels:

Table 6: Geosoft Resistivity Depth Image GDB Data Format

| Channel name | Units | Description |
|---|---|---|
| Xg | metres | UTM Easting WGS84 Zone 14 North |
| Yg | metres | UTM Northing WGS84 Zone 14 North |
| Dist: | metres | Distance from the beginning of the line |
| Depth: | metres | array channel, depth from the surface |
| Z: | metres | array channel, depth from sea level |
| AppRes: | Ohm-m | array channel, Apparent Resistivity |
| TR: | metres | EM system height from sea level |
| Topo: | metres | digital elevation model |
| Radarb: | metres | Calculated EM transmitter-receiver loop terrain clearance from radar altimeter |
| SF: | pV/(A*m^4) | array channel, dB/dT |
| MAG: | nT | TMI data |
| CVG: | nT/m | CVG data |
| DOI: | metres | Depth of Investigation: a measure of VTEM depth effectiveness |
| PLM: | | 60Hz Power Line Monitor |

- Database of the VTEM Waveform "GL170349B_waveform.gdb" in Geosoft GDB format, containing the following channels:

Table 7: Geosoft database for the VTEM waveform

| Channel name | Units | Description |
|---|---|---|
| Time: | milliseconds | Time Channel |
| Tx_Current: | amps | Output current of the transmitter |

- Resistivity Depth Image:

Sections contains apparent resistivity sections along each line in .GRD and .PDF format

Slices contains apparent resistivity slices at selected depths from 25m to depth of investigation, at an increment of 25m in .GRD and .PDF format

Voxel contains 3D Voxel imaging of apparent resistivity data clipped by digital elevation and depth of investigation.

- Grids in Geosoft GRD and GeoTIFF format, as follows:

CVG: Calculated Vertical Derivative (nT/m)
DEM: Digital Elevation Model (metres)
Mag3: Total Magnetic Intensity (nT)
SFz15: dB/dt Z Component Channel 15 (Time Gate 0.02442 ms)
SFz35: dB/dt Z Component Channel 35 (Time Gate 0.3912 ms)
SFz50: dB/dt Z Component Channel 50 (Time Gate 3.12731 ms)
TauSF: dB/dt Z Component, Calculated Time Constant (ms)

A Geosoft .GRD file has a .GI metadata file associated with it, containing grid projection information. A grid cell size of 50 metres was used.

The EM 1D Inversion Models and products have been provided as follows:

- Resistivity-Depth Sections for each survey line (Maps, Grids and geotiffs);
- Resistivity-Depth Slices – 10m increments (Maps, Grids and geotiffs);
- Isopach Maps – Layer Thickness (Maps, Grids and geotiffs);
- 3D Resistivity Depth Voxel for the surveyed block(s).
- 3D Resistivity database in Geosoft format;

Table 1: Survey Specifications EM 1D Inversion Geosoft GDB Data Format

| Channel name | Units | Description |
|---|---|---|
| X | metres | UTM Easting WGS84 Zone 14 North |
| Y | metres | UTM Northing WGS84 Zone 14 North |
| Depth: | meters | array channel, depth from the surface |
| Z: | meters | array channel, depth from sea level |
| Resistivity | Ohm-m | array channel, Inverted Resistivity of the layers |
| Thickness | meters | array channel, Thickness of the layers |
| DEM | meters | digital elevation model |
| Misfit | % | Inversion misfit |
| Nlayers | | Number of layers for the inversion |
| DOI: | metres | Depth of Investigation: merged for RDI database |

# 7. CONCLUSIONS AND RECOMMENDATIONS

A helicopter-borne versatile time domain electromagnetic (VTEM™ ET) geophysical survey has been completed over the Spiritwood-South and Tolna Projects situated near Jamestown and Tolna, North Dakota.

The total area coverage is 2130 km$^2$. Total survey line coverage 3084 line kilometres (3000 km planned). The principal sensors included a Time Domain EM system, and a magnetometer system. Results have been presented as stacked profiles, and contour colour images.

The EM results were converted to 3D resistivity-depth distribution using 1D unconstrained inversion with the GALEI code. 1D inversions have also been performed by Aqua Geo Frameworks LLC using lateral (LCI) and spatial (SCI) constraints and are presented in a separate report. Both sets 1D inversions show a strong correlation with the existing borehole information and were able to map the geological structure in the survey area, specifically Cretaceous basement the overlying Quaternary clay-till overburden with intercalated sand-gravel layers that represent aquifer material.

Respectfully submitted[5],

Zihao Han
**Geotech Ltd.**

Kyle Orlowski
**Geotech Ltd.**

PROFESSIONAL GEOSCIENTIST
KANITA KHALED
PRACTISING MEMBER
2995
ONTARIO

PROFESSIONAL GEOSCIENTIST
JEAN M. LEGAULT
PRACTISING MEMBER
0948
ONTARIO

Kanita Khaled, P. Geo.
**Geotech Ltd.**

Jen M. Legault, M.Sc.A., P.Eng, P.Geo
**Geotech Ltd.**

June 2019

[5] Final data processing of the EM and magnetic data were carried out by Zihao Han, from the office of Geotech Ltd. in Aurora, Ontario, under the supervision of Kanita Khaled, P.Geo.

# APPENDIX A

## SURVEY AREA LOCATION MAP

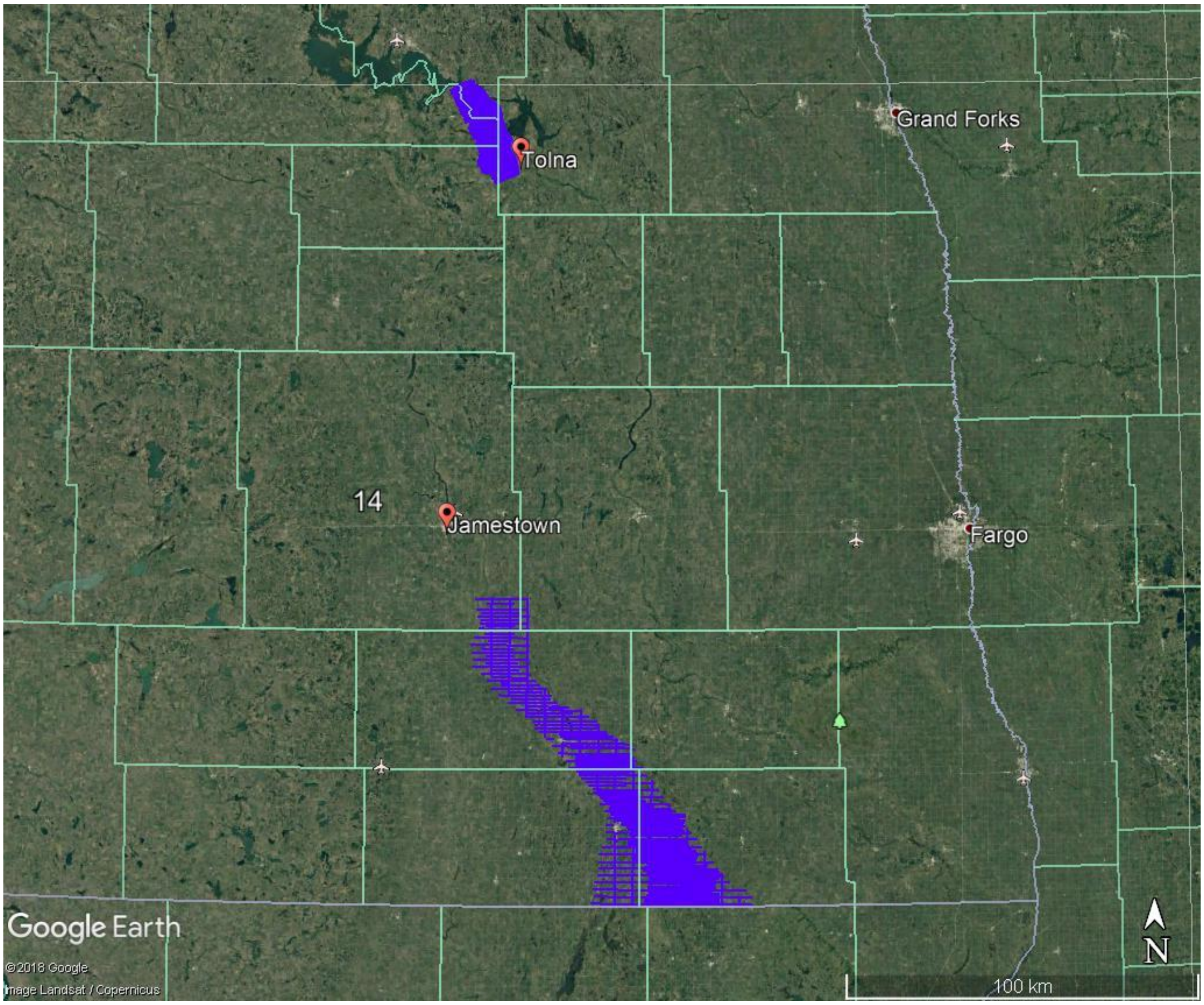


Overview of the Survey Area

# APPENDIX B

## SURVEY AREA COORDINATES

| Spiritwood | |
|---|---|
| WGS84 UTM Zone 14N | |
| X | Y |
| 545351 | 5172438 |
| 533015 | 5172419 |
| 532933 | 5164035 |
| 533353 | 5153716 |
| 542701 | 5143090 |
| 554971 | 5129275 |
| 553449 | 5133723 |
| 553444 | 5134056 |
| 553573 | 5134109 |
| 553587 | 5134624 |
| 553910 | 5134994 |
| 554835 | 5134811 |
| 555011 | 5134753 |
| 555014 | 5133600 |
| 554793 | 5133544 |
| 554666 | 5133319 |
| 554264 | 5133378 |
| 554153 | 5133661 |
| 553449 | 5133723 |
| 554971 | 5129275 |
| 565951 | 5118171 |
| 565885 | 5106981 |
| 569262 | 5109845 |
| 569323 | 5110060 |
| | |

| Spiritwood | |
|---|---|
| WGS84 UTM Zone 14N | |
| X | Y |
| 569694 | 5110173 |
| 570113 | 5111464 |
| 571233 | 5111493 |
| 571257 | 5111140 |
| 571521 | 5111103 |
| 571380 | 5110597 |
| 571440 | 5110047 |
| 571264 | 5109543 |
| 570821 | 5109090 |
| 570754 | 5109052 |
| 570479 | 5108326 |
| 569738 | 5108339 |
| 569445 | 5109155 |
| 569451 | 5109650 |
| 569270 | 5109830 |
| 569262 | 5109845 |
| 565885 | 5106981 |
| 566074 | 5101306 |
| 566105 | 5087428 |
| 607007 | 5088130 |
| 587779 | 5112528 |
| 573957 | 5131000 |
| 561908 | 5140783 |
| 545342 | 5156322 |
| 545351 | 5172438 |

| Tolna | |
|---|---|
| WGS84 UTM Zone 14N | |
| X | Y |
| 527500 | 5317701 |
| 522897 | 5315805 |
| 521841 | 5314811 |
| 526382 | 5305667 |
| 527981 | 5305687 |
| 526915 | 5304662 |
| 528637 | 5301095 |
| 529498 | 5300829 |
| 529088 | 5300091 |
| 530339 | 5297548 |
| 529662 | 5294781 |
| 529970 | 5293735 |
| 530626 | 5293366 |
| 530708 | 5292177 |
| 531466 | 5291870 |
| 532020 | 5291460 |
| 533312 | 5291439 |
| 534788 | 5288384 |
| 541451 | 5291111 |
| 541451 | 5291767 |
| 541369 | 5292936 |
| 541307 | 5293469 |
| 541082 | 5294022 |
| 540877 | 5296421 |
| | |

| Tolna | |
|---|---|
| WGS84 UTM Zone 14N | |
| X | Y |
| 540610 | 5296892 |
| 540774 | 5298164 |
| 540549 | 5298717 |
| 540590 | 5299312 |
| 540528 | 5299906 |
| 539934 | 5300911 |
| 539544 | 5301321 |
| 538170 | 5303207 |
| 537084 | 5305810 |
| 536612 | 5308681 |
| 535997 | 5309644 |
| 535936 | 5310218 |
| 535731 | 5310751 |
| 534808 | 5311592 |
| 532943 | 5312658 |
| 532738 | 5313129 |
| 532225 | 5314155 |
| 530626 | 5315364 |
| 530359 | 5315836 |
| 529847 | 5316266 |
| 529109 | 5316533 |
| 528842 | 5317004 |
| 528924 | 5317722 |
| 527500 | 5317701 |
| | |

## APPENDIX C - GEOPHYSICAL MAPS[1]

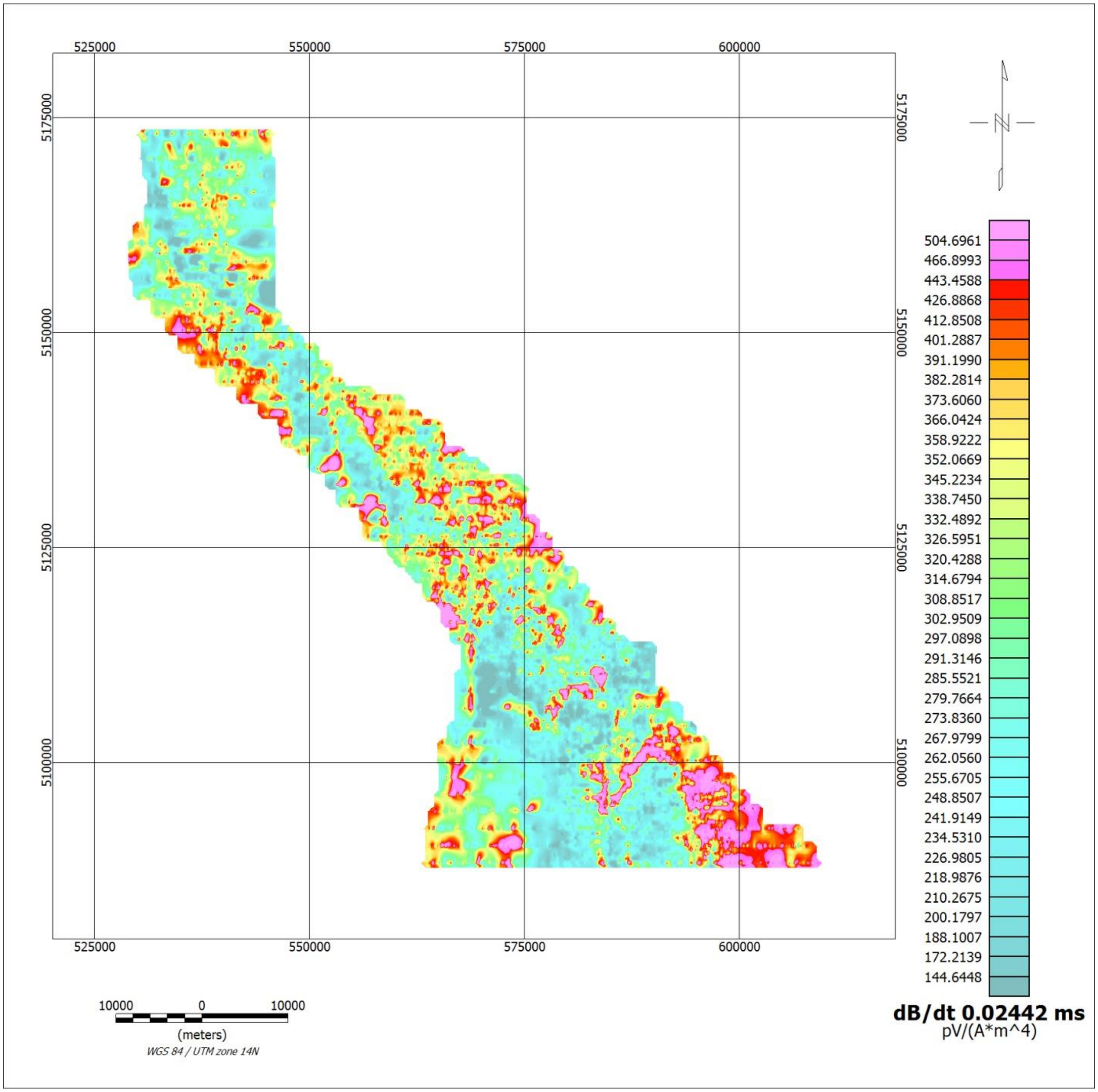


Spiritwood-South: VTEM dB/dt Z Component Channel 15, Time Gate 0.02442 ms

[1] Complete full size geophysical maps are also available in PDF format located in the final data maps folder

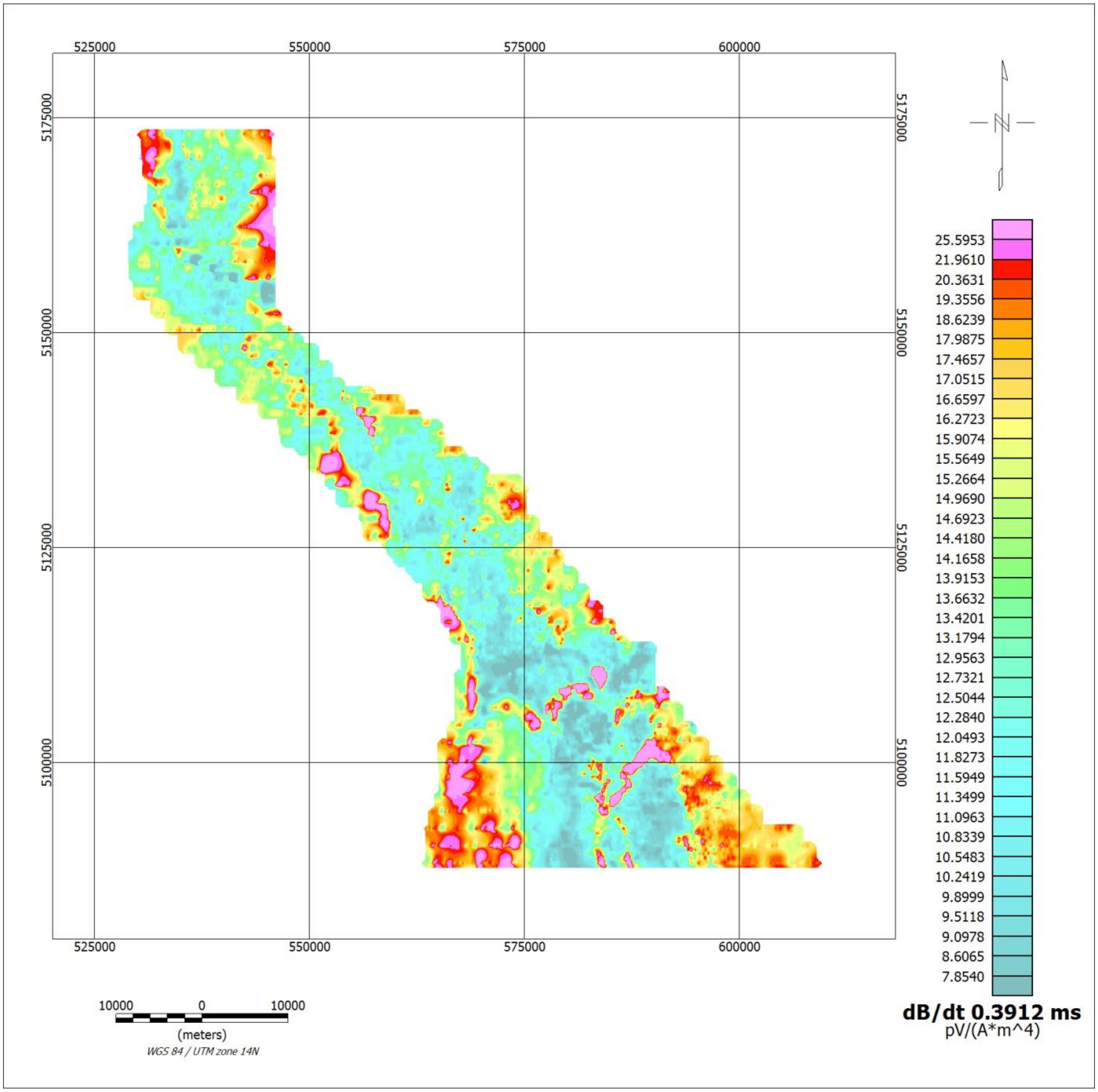


Spiritwood-South: VTEM dB/dt Z Component Channel 35, Time Gate 0.3912 ms

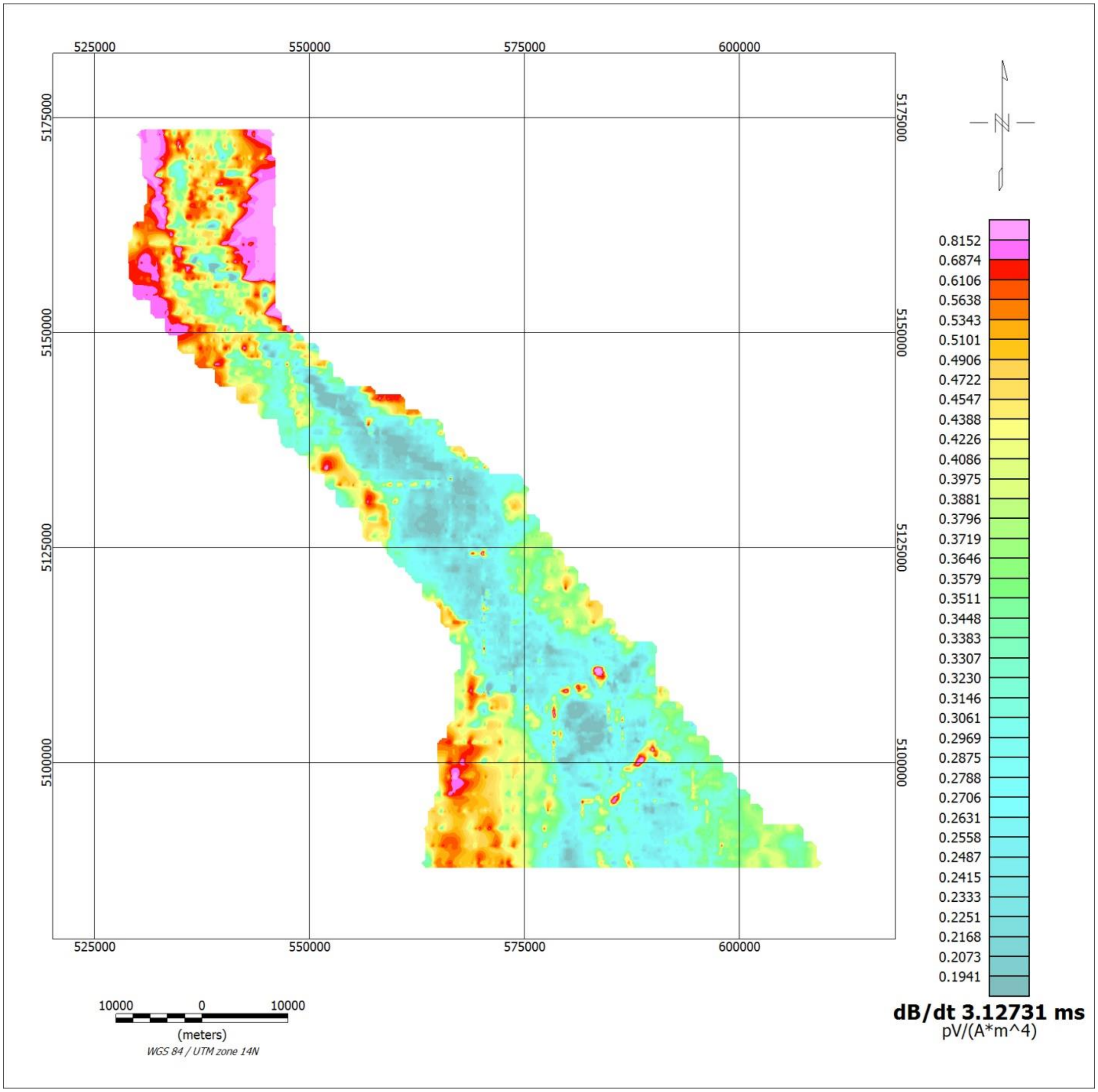


Spiritwood-South: VTEM dB/dt Z Component, Channel 50, Time Gate 3.12731 ms

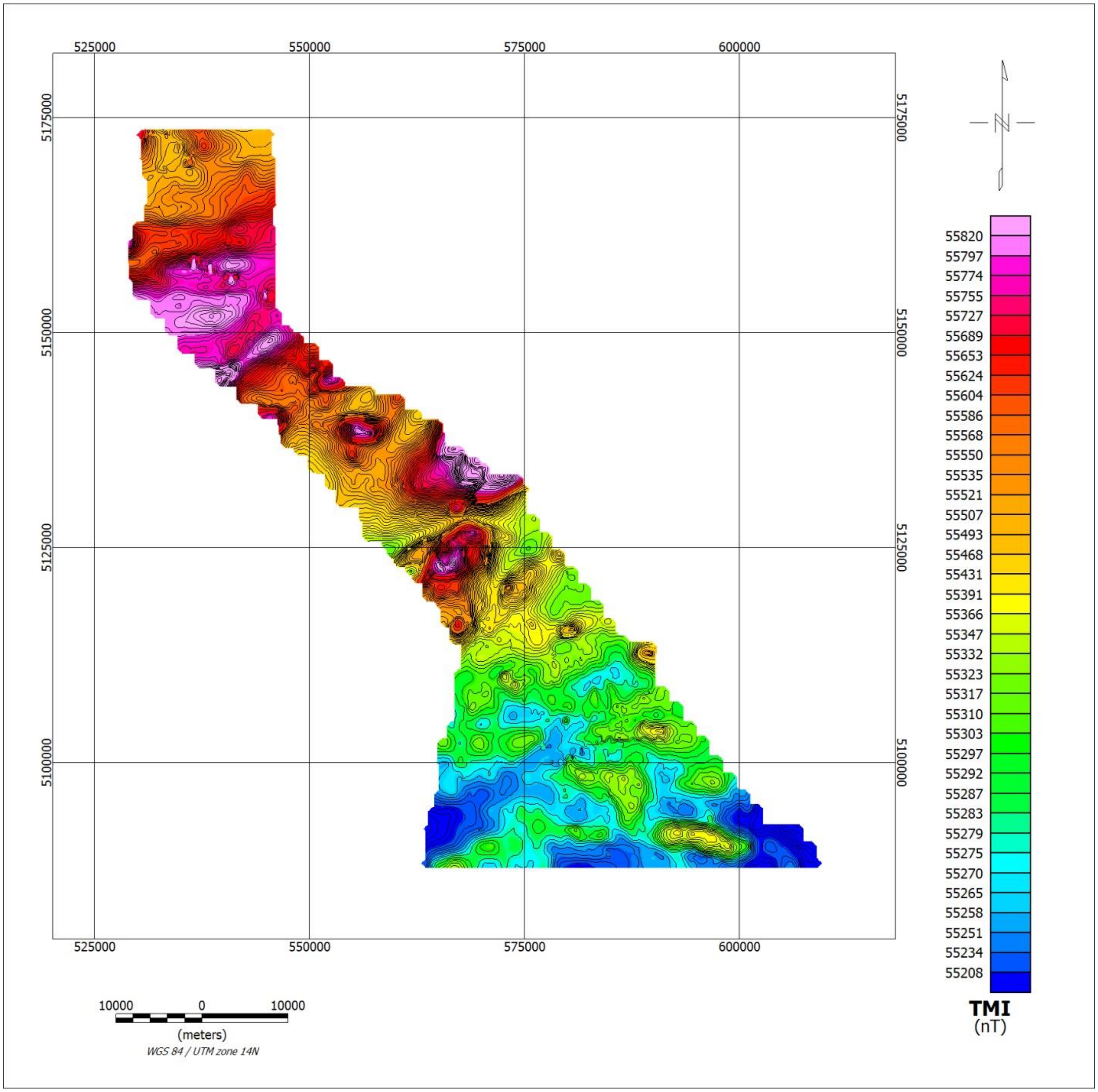


Spiritwood-South: Total Magnetic Intensity (TMI) and contours

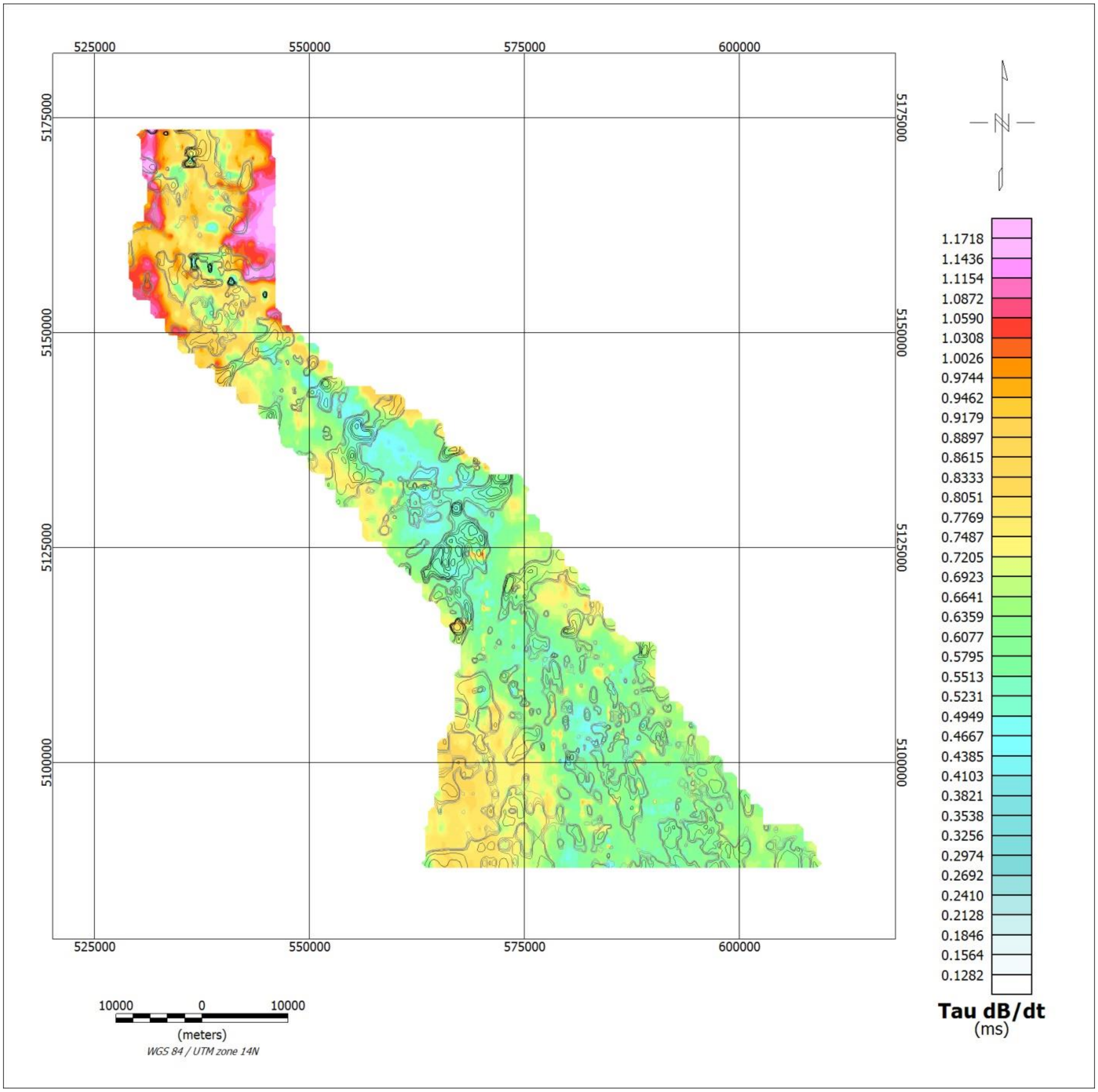


Spiritwood-South: dB/dt Calculated Time Constant (Tau) with Calculated Vertical Derivative contours

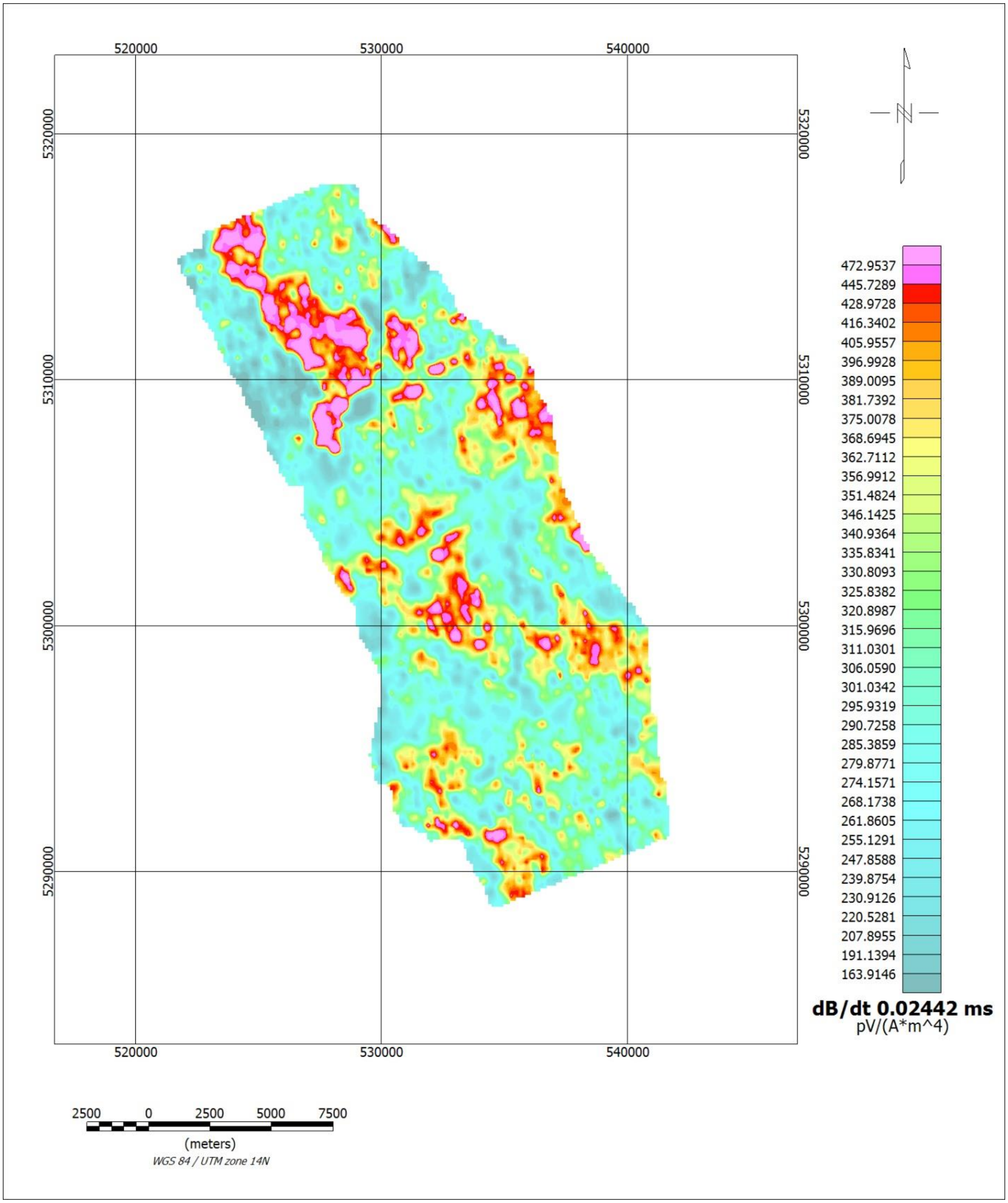


Tolna: VTEM dB/dt Z Component Channel 15, Time Gate 0.02442 ms

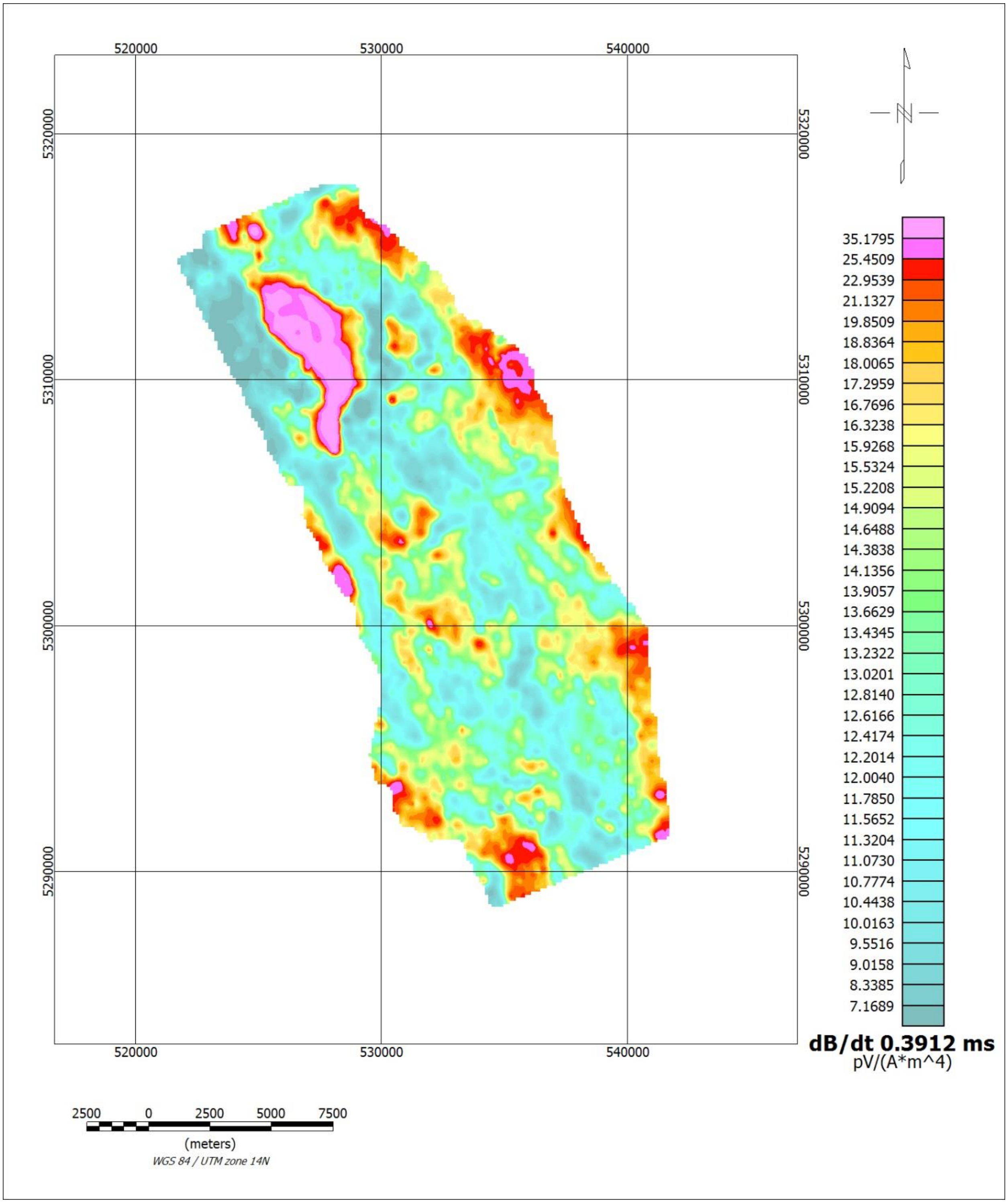


Tolna: VTEM dB/dt Z Component Channel 35, Time Gate 0.3912 ms

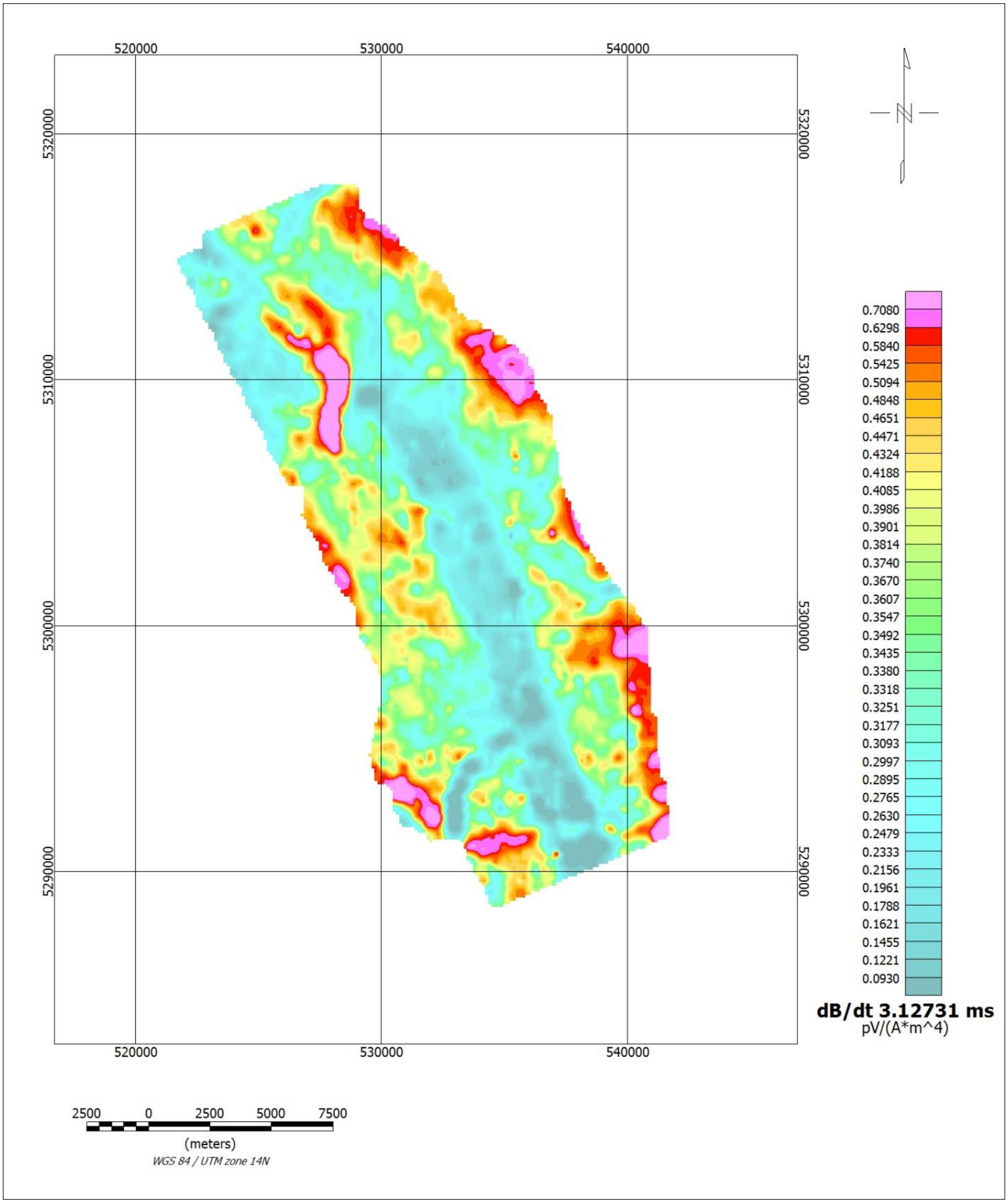


Tolna: VTEM dB/dt Z Component, Channel 50, Time Gate 3.12731 ms

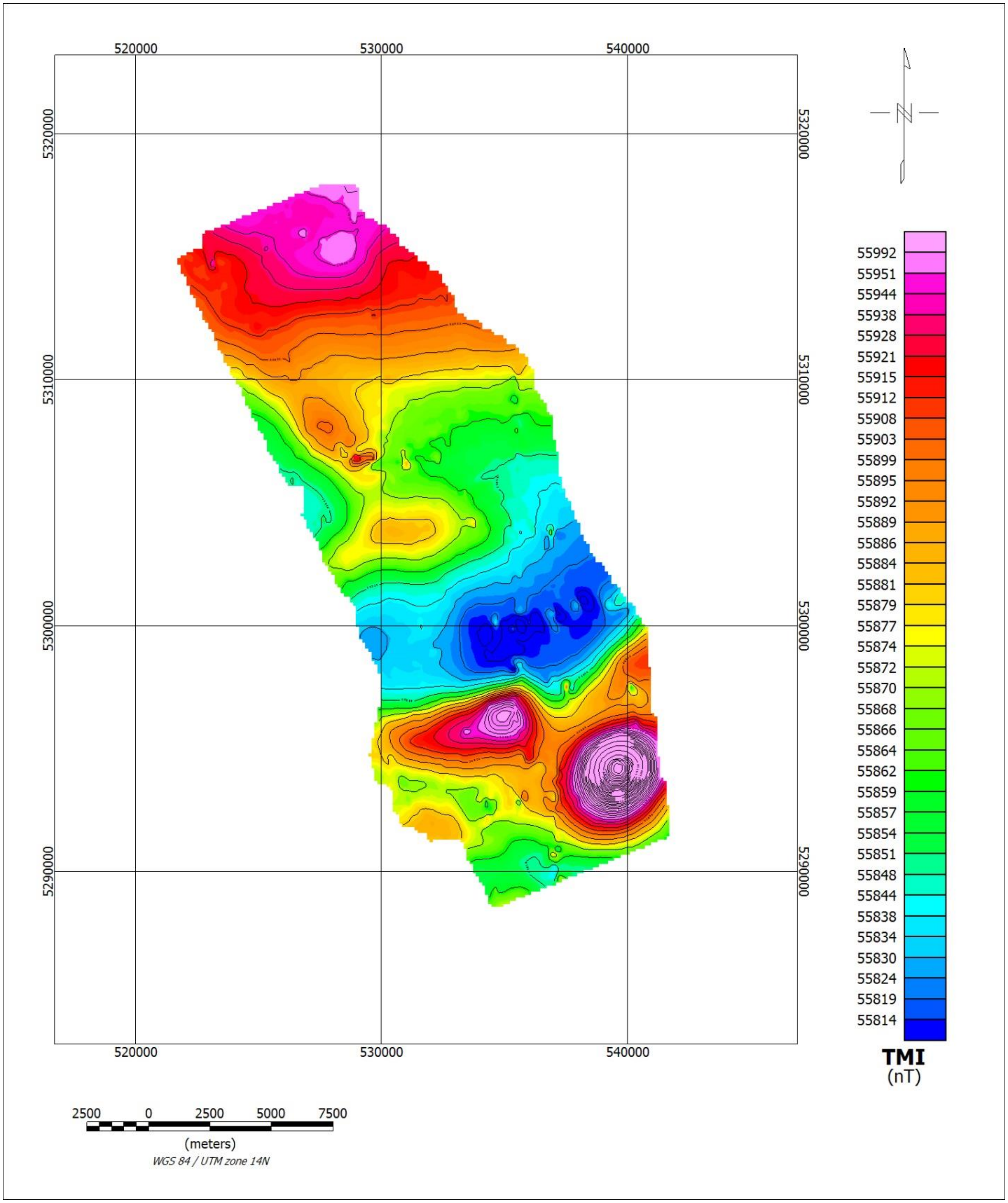


Tolna: Total Magnetic Intensity (TMI) grid and contours

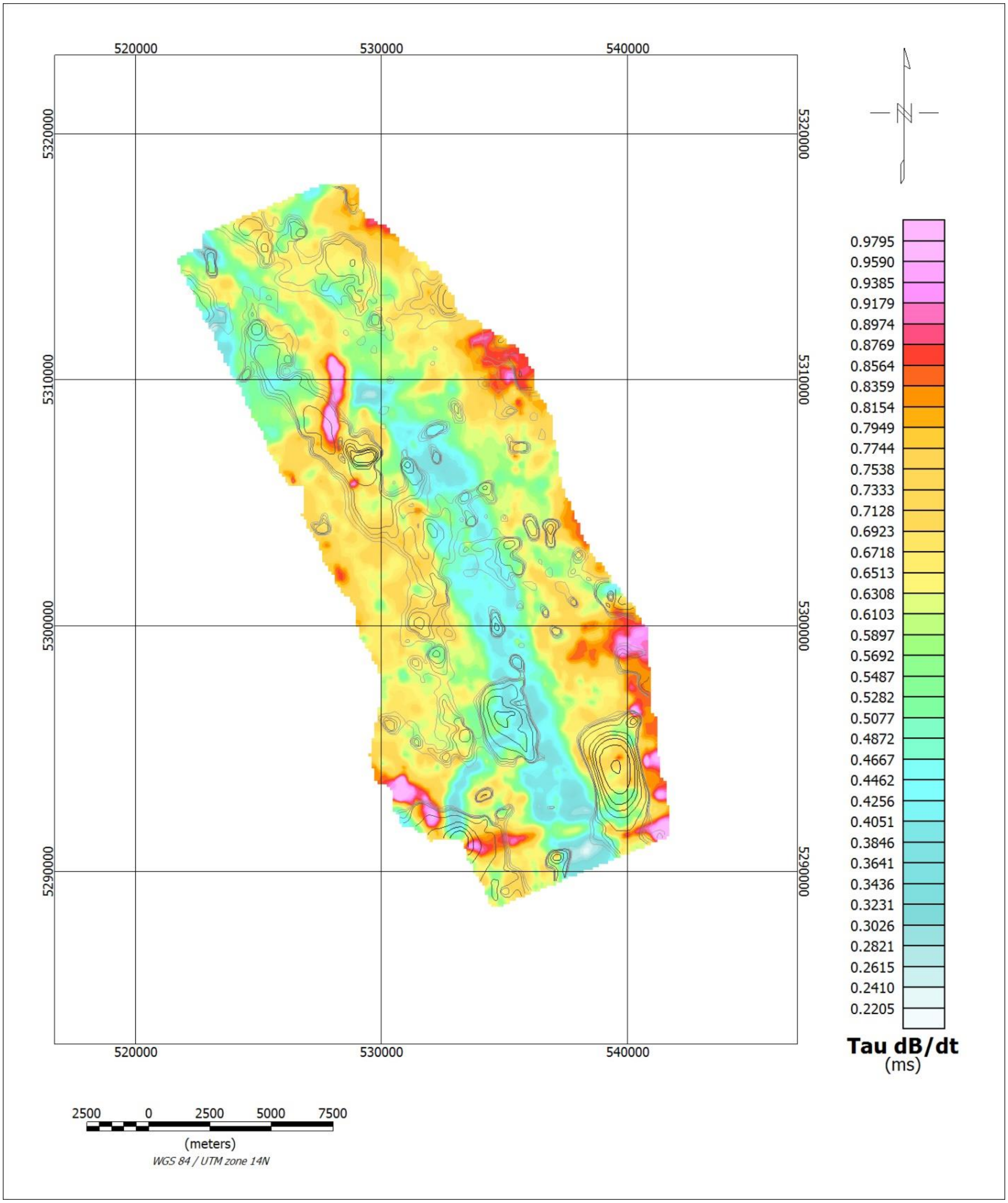


Tolna: dB/dt Calculated Time Constant (Tau) with Calculated Vertical Derivative contours

## RESISTIVITY DEPTH IMAGE (RDI) MAPS

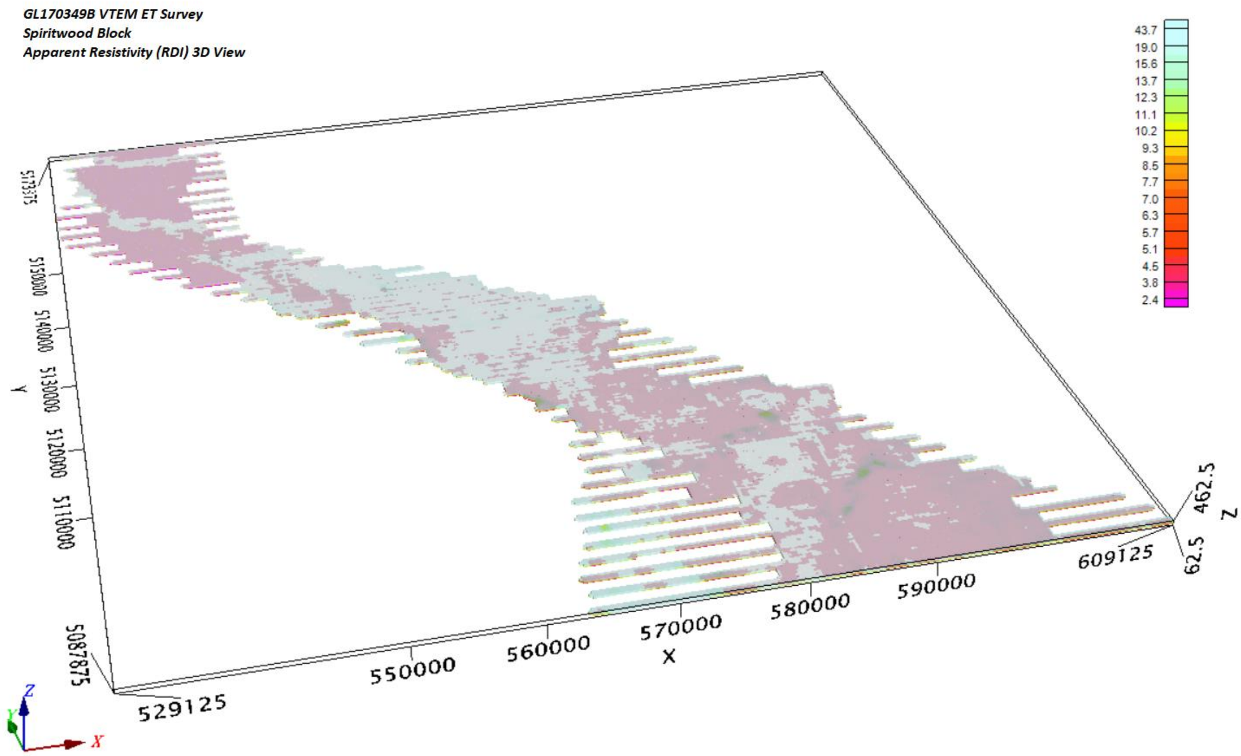


Spiritwood-South: 3D View of Resistivity-Depth Image (RDI) Voxel (units in ohm-m)

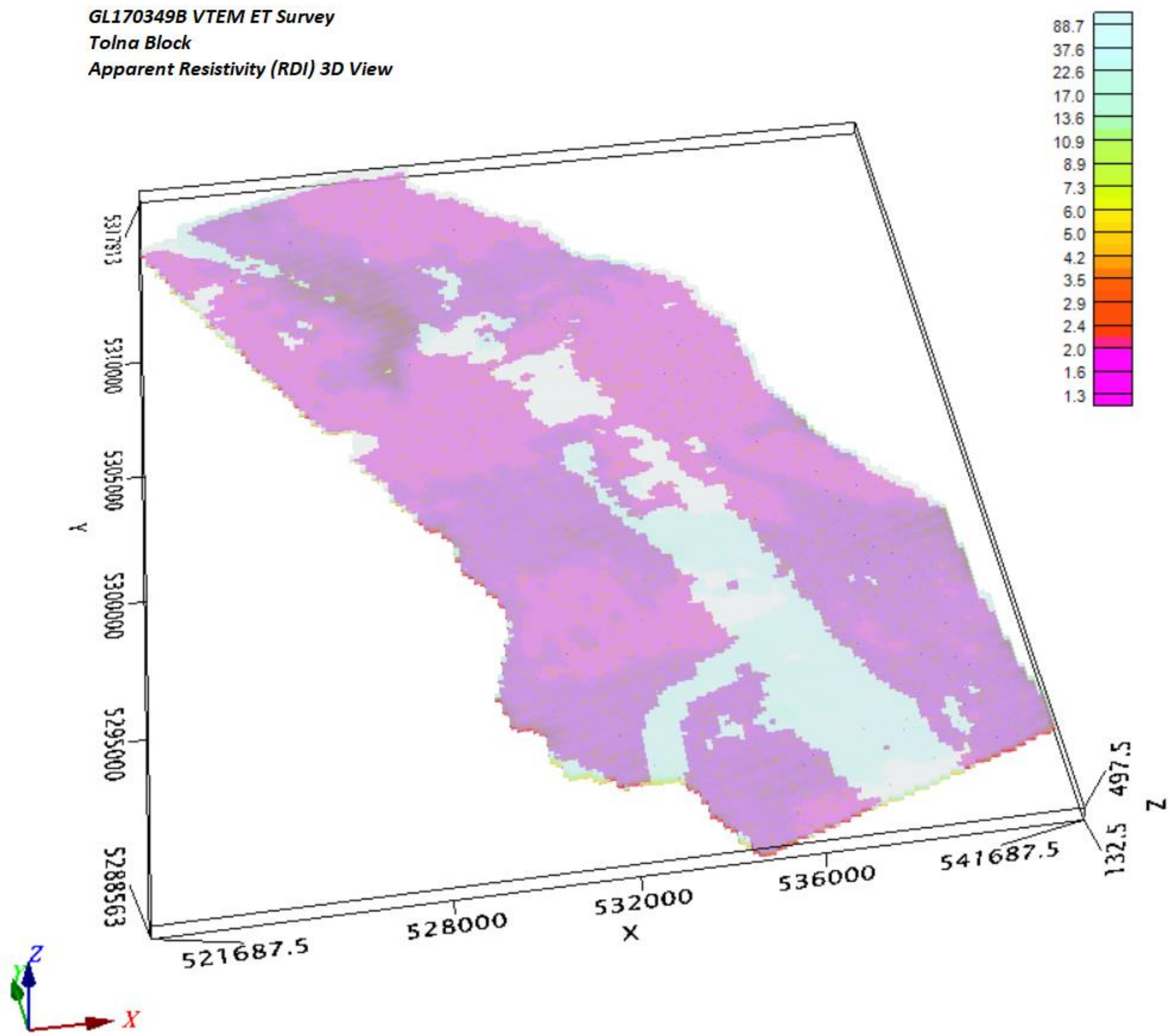


Tolna: 3D View of Resistivity-Depth Image (RDI) Voxel (units in ohm-m)

# APPENDIX D

## GENERALIZED MODELING RESULTS OF THE VTEM SYSTEM

## INTRODUCTION

The VTEM system is based on a concentric or central loop design, whereby, the receiver is positioned at the centre of a transmitter loop that produces a primary field. The wave form is a bi-polar, modified square wave with a turn-on and turn-off at each end.

During turn-on and turn-off, a time varying field is produced (dB/dt) and an electro-motive force (emf) is created as a finite impulse response. A current ring around the transmitter loop moves outward and downward as time progresses. When conductive rocks and mineralization are encountered, a secondary field is created by mutual induction and measured by the receiver at the centre of the transmitter loop.

Efficient modeling of the results can be carried out on regularly shaped geometries, thus yielding close approximations to the parameters of the measured targets. The following is a description of a series of common models made for the purpose of promoting a general understanding of the measured results.

A set of models has been produced for the Geotech VTEM® system dB/dT Z and X components (see models D1 to D15). The Maxwell ™ modeling program (EMIT Technology Pty. Ltd. Midland, WA, AU) used to generate the following responses assumes a resistive half-space. The reader is encouraged to review these models, so as to get a general understanding of the responses as they apply to survey results. While these models do not begin to cover all possibilities, they give a general perspective on the simple and most commonly encountered anomalies.

As the plate dips and departs from the vertical position, the peaks become asymmetrical.

As the dip increases, the aspect ratio (Min/Max) decreases and this aspect ratio can be used as an empirical guide to dip angles from near 90º to about 30º. The method is not sensitive enough where dips are less than about 30º.

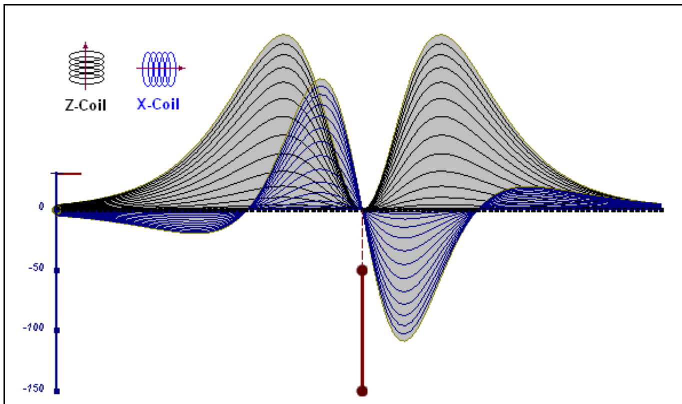


**Figure D-1**: vertical thin plate

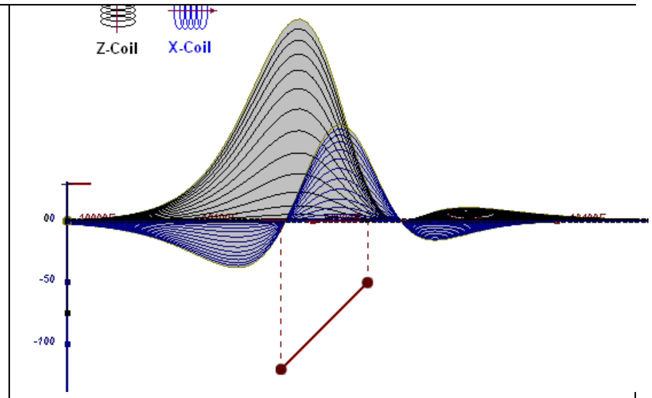


**Figure D-2**: inclined thin plate

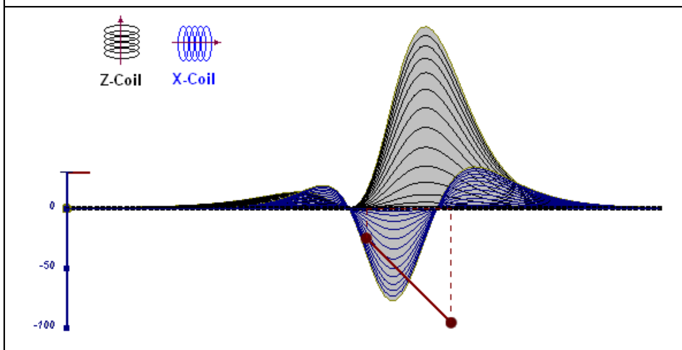


**Figure D-3**: inclined thin plate

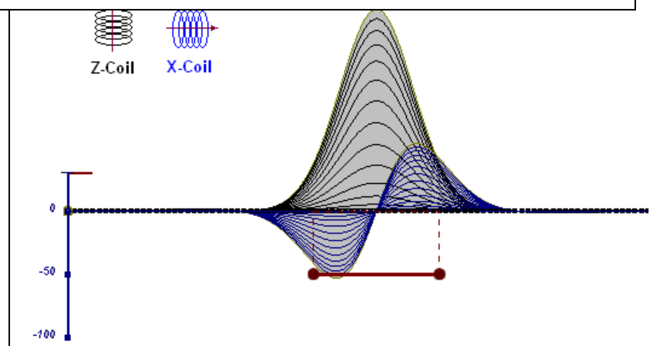


**Figure D-4**: horizontal thin plate

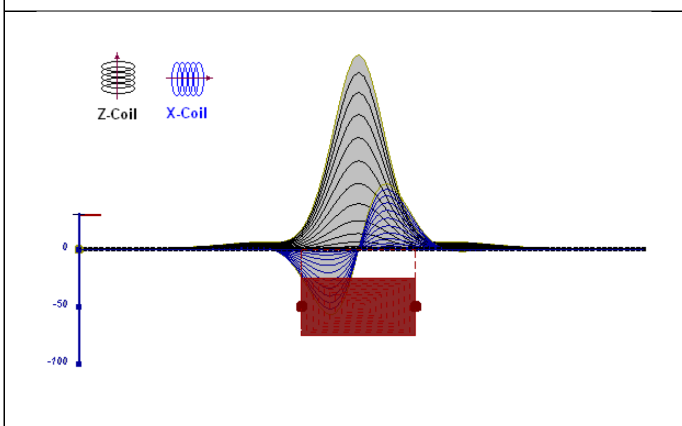


**Figure D-5**: horizontal thick plate (linear scale of the response)

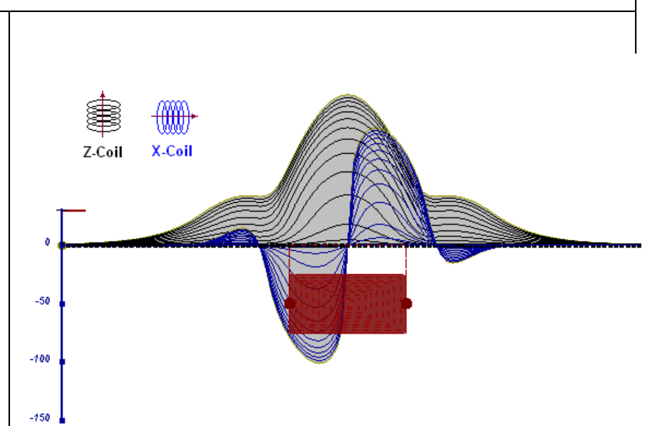


**Figure D-6**: horizontal thick plate (log scale of the response)

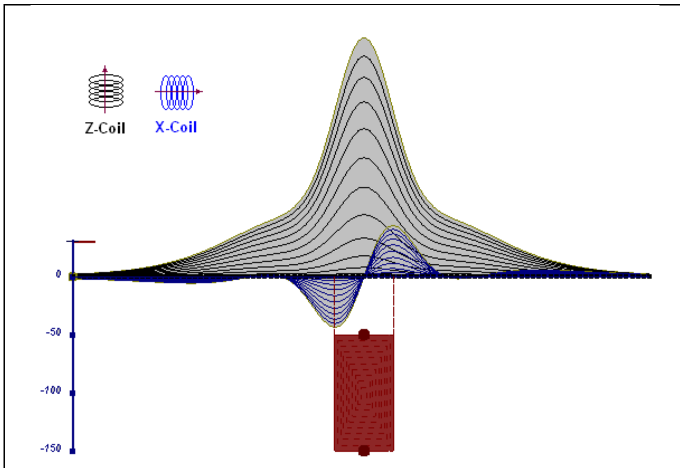


**Figure D-7**: vertical thick plate (linear scale of the response). 50 m depth

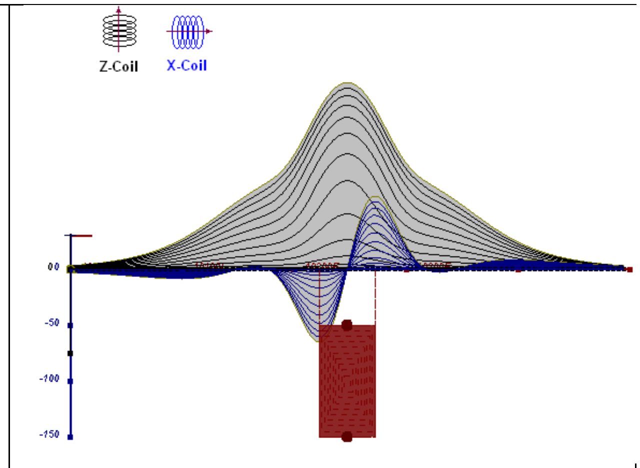


**Figure D-8**: vertical thick plate (log scale of the response). 50 m depth

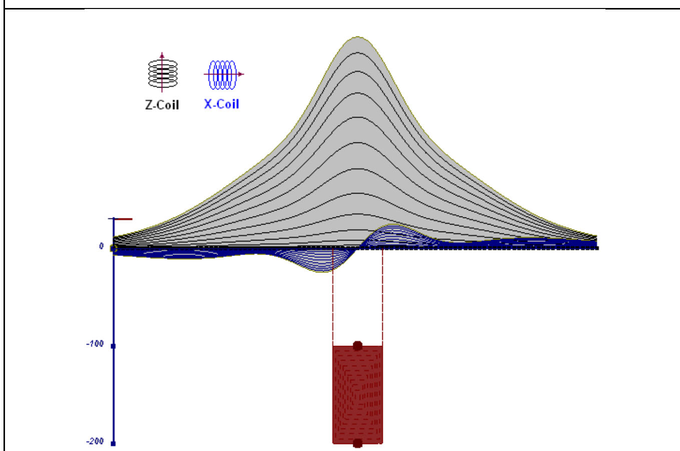


**Figure D-9**: vertical thick plate (linear scale of the response). 100 m depth

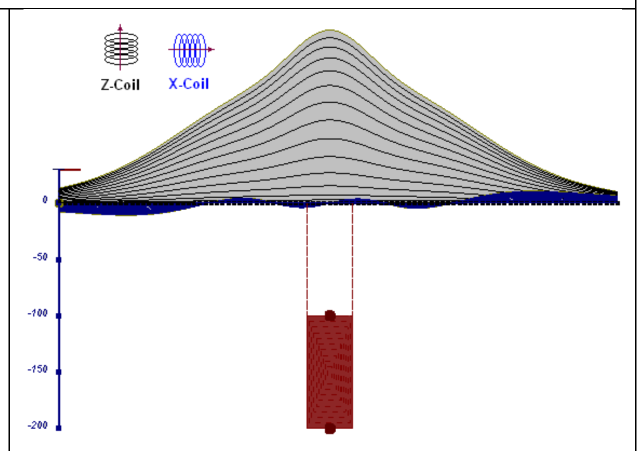


**Figure D-10**: vertical thick plate (linear scale of the response). Depth / horizontal thickness=2.5

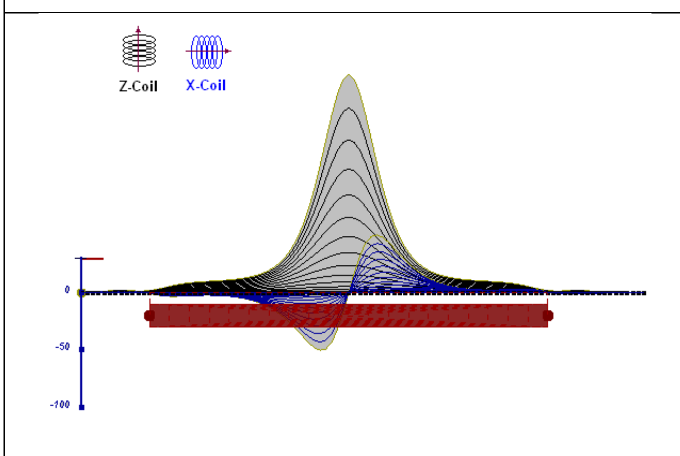


**Figure D-11**: horizontal thick plate (linear scale of the response)

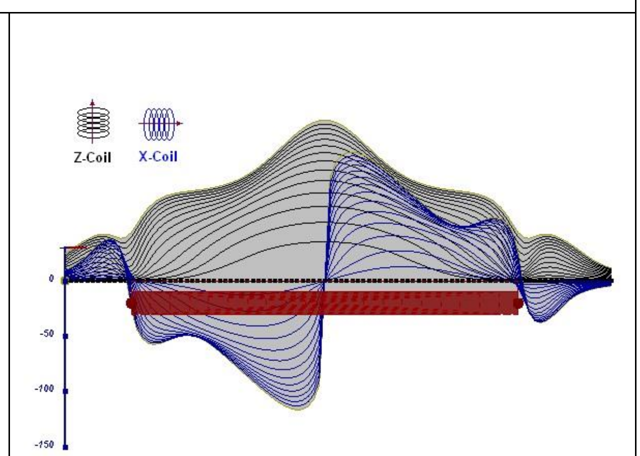


**Figure D-12**: horizontal thick plate (log scale of the response)

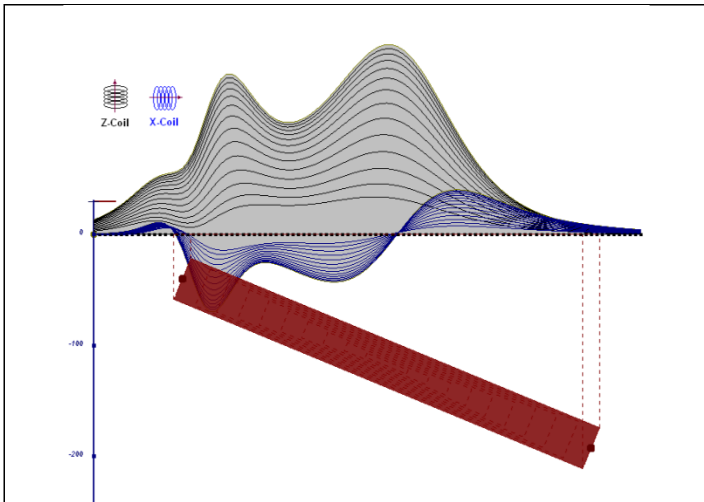


**Figure D-13**: inclined long thick plate

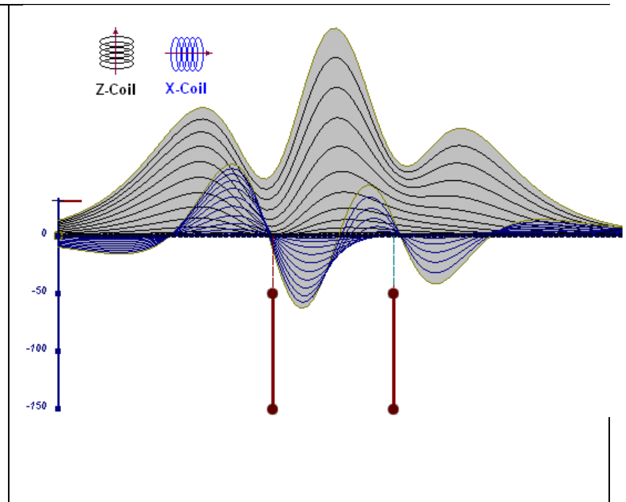


**Figure D-14**: two vertical thin plates

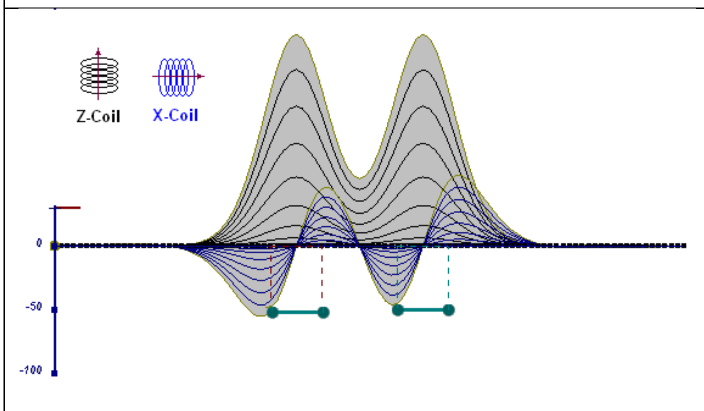


**Figure D-15**: two horizontal thin plates

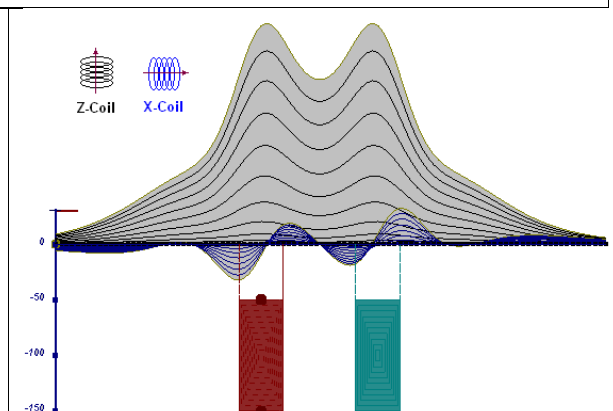


**Figure D-16**: two vertical thick plates

The same type of target but with different thickness, for example, creates different form of the response:

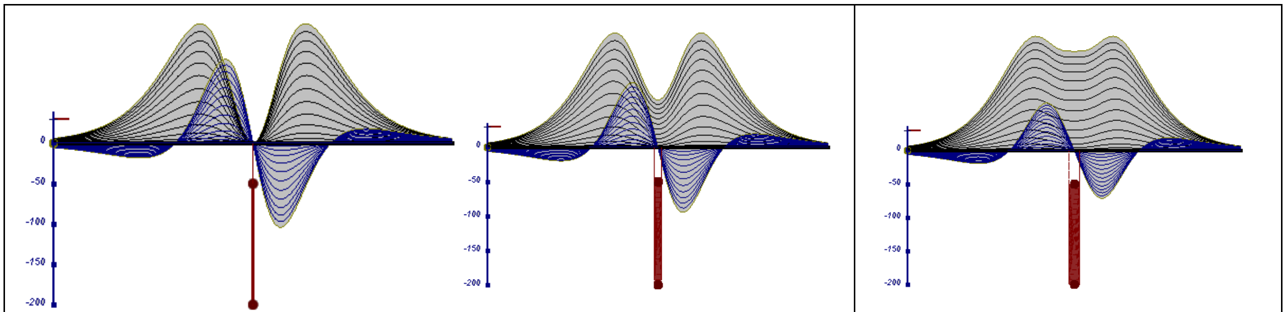

"thin" | 10 m thickness | 15 m thickness

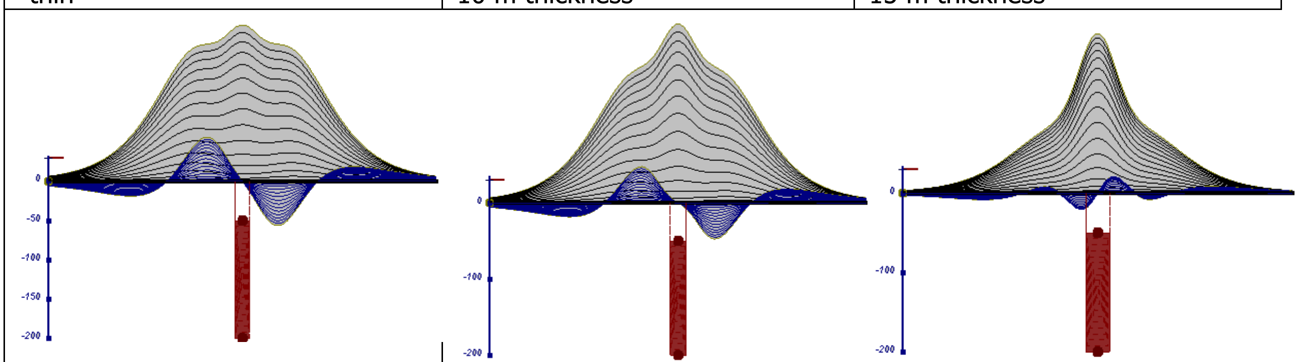

18 m thickness | 20 m thickness | 30 m thickness

**Figure D-17**: Conductive vertical plate, depth 50 m, strike length 200 m, depth extends 150 m.

Alexander Prikhodko, PhD, P.Geo
**Geotech Ltd.**

September 2010

# APPENDIX E

## EM TIME CONSTANT (TAU) ANALYSIS

Estimation of time constant parameter[1] in transient electromagnetic method is one of the steps toward the extraction of the information about conductances beneath the surface from TEM measurements.

The most reliable method to discriminate or rank conductors from overburden, background or one and other is by calculating the EM field decay time constant (TAU parameter), which directly depends on conductance despite their depth and accordingly amplitude of the response.

## THEORY

As established in electromagnetic theory, the magnitude of the electro-motive force (emf) induced is proportional to the time rate of change of primary magnetic field at the conductor. This emf causes eddy currents to flow in the conductor with a characteristic transient decay, whose Time Constant (Tau) is a function of the conductance of the survey target or conductivity and geometry (including dimensions) of the target. The decaying currents generate a proportional secondary magnetic field, the time rate of change of which is measured by the receiver coil as induced voltage during the Off time.

The receiver coil output voltage (**$e_0$**) is proportional to the time rate of change of the secondary magnetic field and has the form,

$$e_0 \propto (1 / \tau)\, e^{-(t/\tau)}$$

Where,
$\tau$ = L/R is the characteristic time constant of the target (TAU)
R = resistance
L = inductance

From the expression, conductive targets that have small value of resistance and hence large value of $\tau$ yield signals with small initial amplitude that decays relatively slowly with progress of time. Conversely, signals from poorly conducting targets that have large resistance value and small $\tau$, have high initial amplitude but decay rapidly with time[1] (Fig. E1).

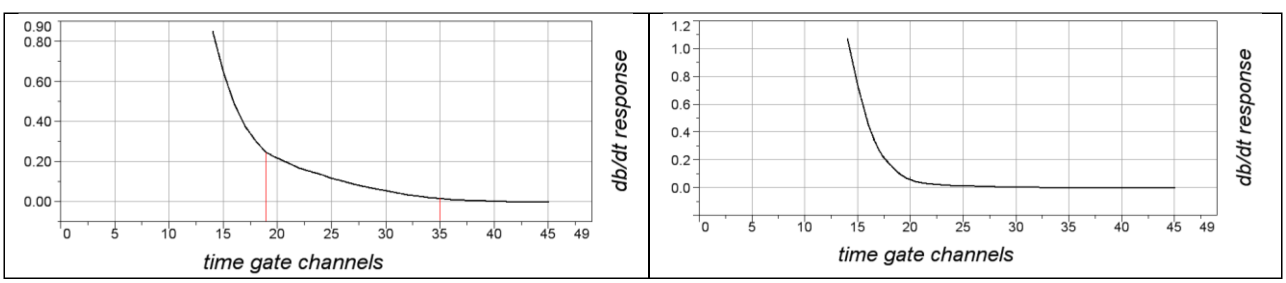


Figure E-1: Left – presence of good conductor, right – poor conductor.

---

[1] McNeill, JD, 1980, "Applications of Transient Electromagnetic Techniques", Technical Note TN-7 page 5, Geonics Limited, Mississauga, Ontario.

## EM Time Constant (Tau) Calculation

The EM Time-Constant (TAU) is a general measure of the speed of decay of the electromagnetic response and indicates the presence of eddy currents in conductive sources as well as reflecting the "conductance quality" of a source. Although TAU can be calculated using either the measured dB/dt decay or the calculated B-field decay, dB/dt is commonly preferred due to better stability (S/N) relating to signal noise. Generally, TAU calculated on base of early time response reflects both near surface overburden and poor conductors whereas, in the late ranges of time, deep and more conductive sources, respectively. For example early time TAU distribution in an area that indicates conductive overburden is shown in Figure 2.

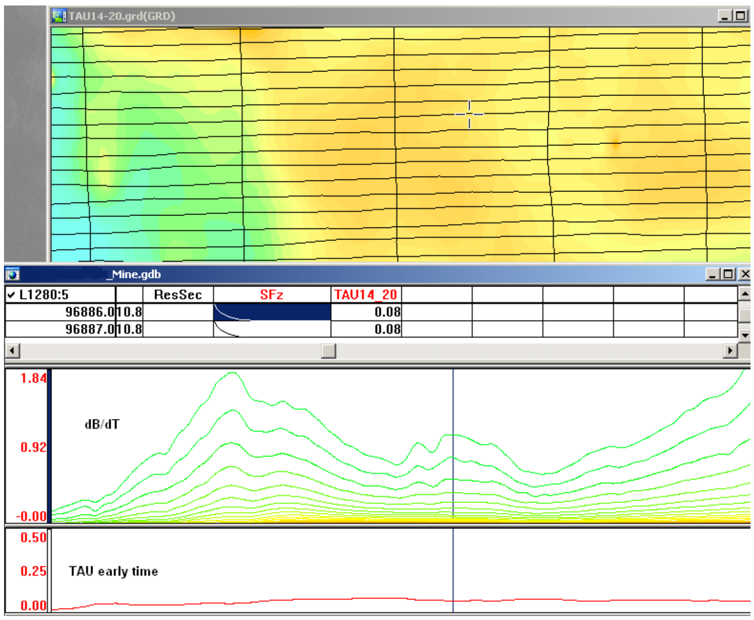


Figure E-2: Map of early time TAU. Area with overburden conductive layer and local sources.

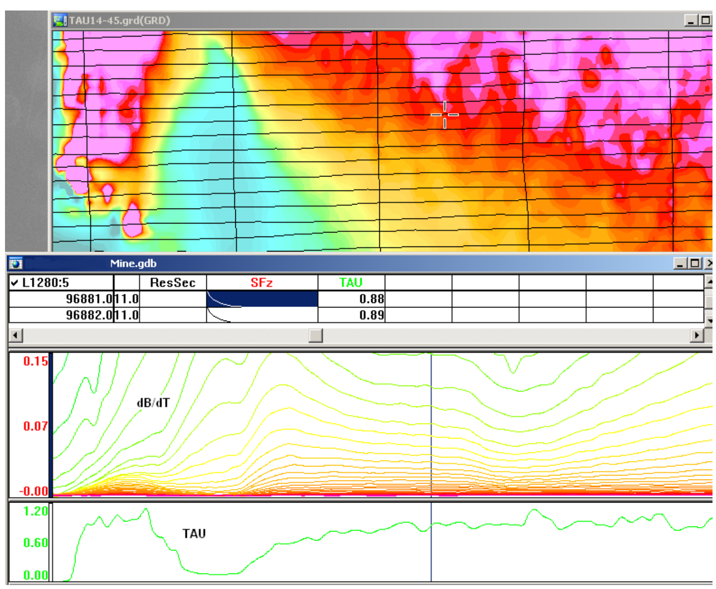


Figure E-3: Map of full time range TAU with EM anomaly due to deep highly conductive target.

There are many advantages of TAU maps:

- TAU depends only on one parameter (conductance) in contrast to response magnitude;
- TAU is integral parameter, which covers time range and all conductive zones and targets are displayed independently of their depth and conductivity on a single map.
- Very good differential resolution in complex conductive places with many sources with different conductivity.
- Signs of the presence of good conductive targets are amplified and emphasized independently of their depth and level of response accordingly.

In the example shown in Figure 4 and 5, three local targets are defined, each of them with a different depth of burial, as indicated on the resistivity depth image (RDI). All are very good conductors but the deeper target (number 2) has a relatively weak dB/dt signal yet also features the strongest total TAU (Figure 4). This example highlights the benefit of TAU analysis in terms of an additional target discrimination tool.

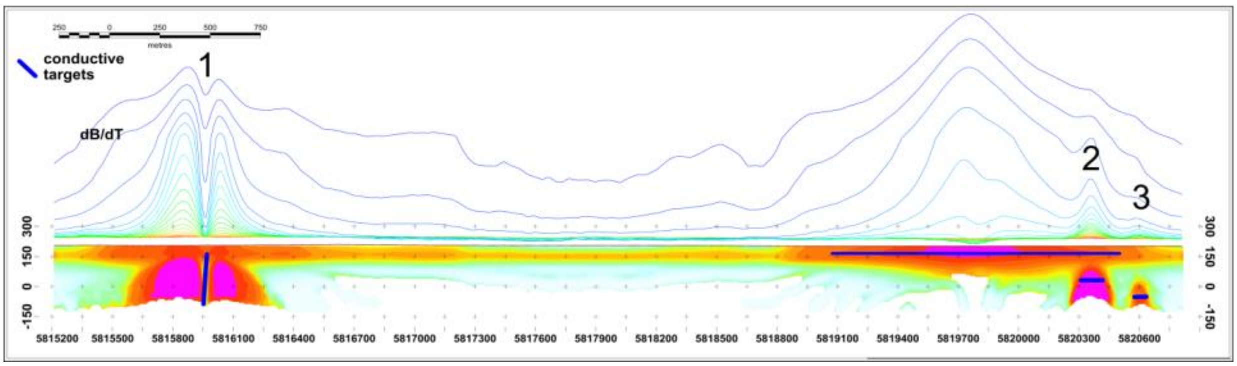


Figure E-4: dB/dt profile and RDI with different depths of targets.

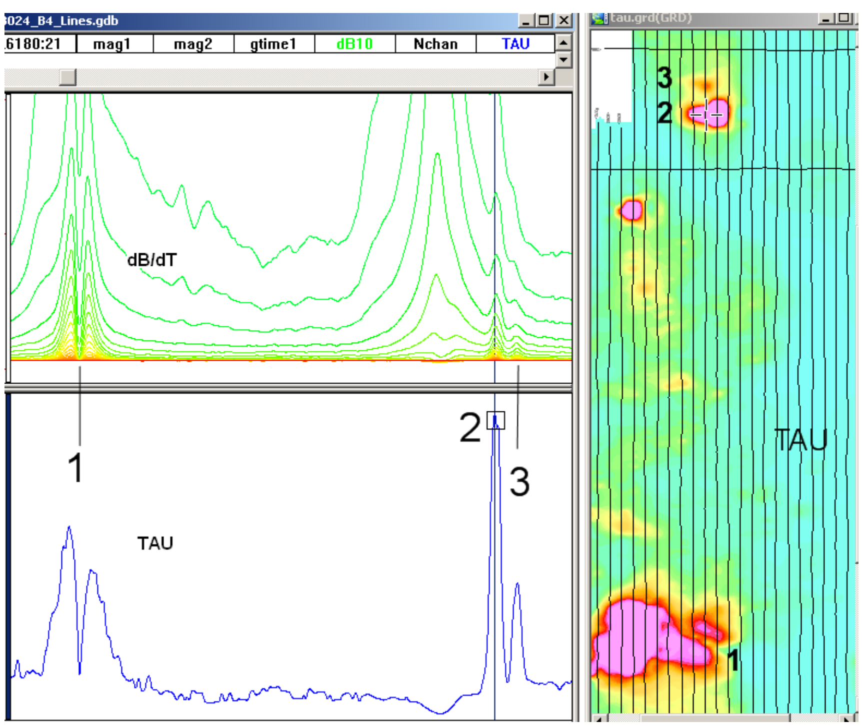


Figure E-5: Map of total TAU and dB/dt profile.

The EM Time Constants for dB/dt and B-field were calculated using the "sliding Tau" in-house program developed at Geotech[2]. The principle of the calculation is based on using of time window (4 time channels) which is sliding along the curve decay and looking for latest time channels which have a response above the level of noise and decay. The EM decays are obtained from all available decay channels, starting at the latest channel. Time constants are taken from a least square fit of a straight-line (log/linear space) over the last 4 gates above a pre-set signal threshold level (Figure F6). Threshold settings are pointed in the "label" property of TAU database channels. The sliding Tau method determines that, as the amplitudes increase, the time-constant is taken at progressively later times in the EM decay. Conversely, as the amplitudes decrease, Tau is taken at progressively earlier times in the decay. If the maximum signal amplitude falls below the threshold, or becomes negative for any of the 4 time gates, then Tau is not calculated and is assigned a value of "dummy" by default.

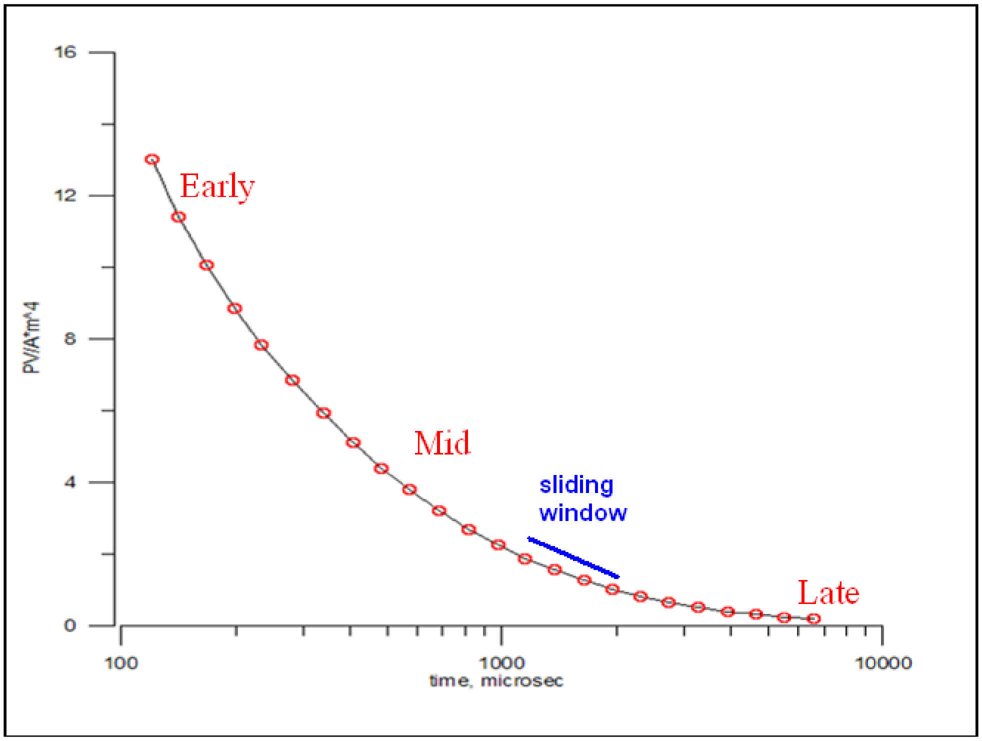


Figure E-6: Typical dB/dt decays of VTEM data

Alexander Prikhodko, PhD, P.Geo
**Geotech Ltd.**

September 2010

[2] by A. Prikhodko

# APPENDIX F

## TEM RESISTIVITY DEPTH IMAGING (RDI)

Resistivity depth imaging (RDI) is technique used to rapidly convert EM profile decay data into an equivalent resistivity versus depth cross-section, by deconvolving the measured TEM data.
The used RDI algorithm of Resistivity-Depth transformation is based on scheme of the apparent resistivity transform of Maxwell A. Meju (1998)[1] and TEM response from conductive half-space. The program is developed by Alexander Prikhodko and depth calibrated based on forward plate modeling for VTEM system configuration (Fig. 1-10).

RDIs provide reasonable indications of conductor relative depth and vertical extent, as well as accurate 1D layered-earth apparent conductivity/resistivity structure across VTEM flight lines. Approximate depth of investigation of a TEM system, image of secondary field distribution in half space, effective resistivity, initial geometry and position of conductive targets is the information obtained on base of the RDIs.

Maxwell forward modeling with RDI sections from the synthetic responses (VTEM system).

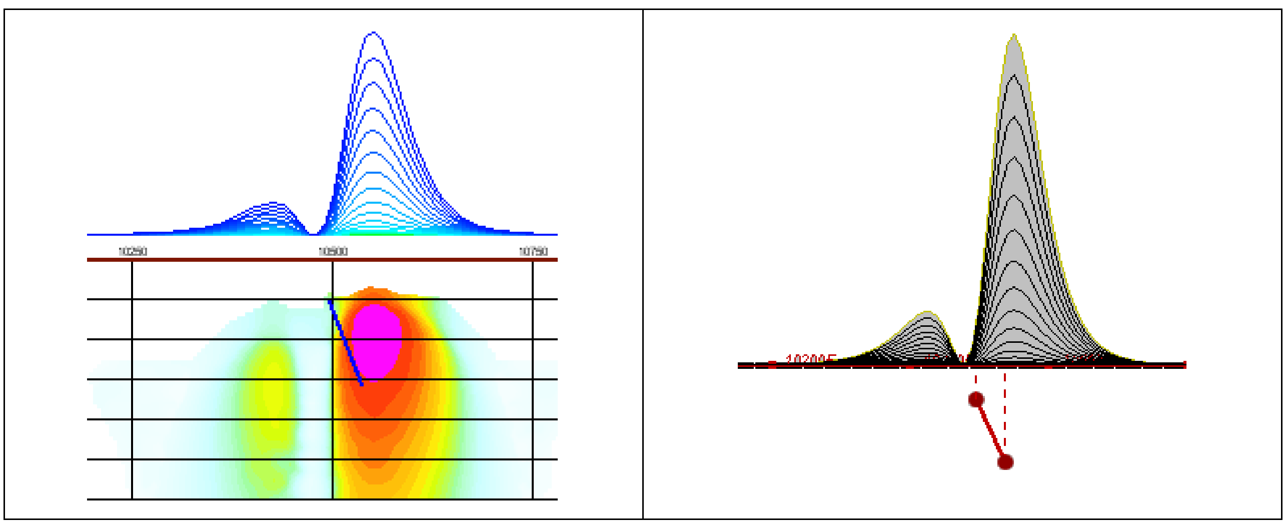

Figure F-1: Maxwell plate model and RDI from the calculated response for conductive "thin" plate (depth 50 m, dip 65 degree, depth extend 100 m).

[1] Maxwell A. Meju, 1998, Short Note: A simple method of transient electromagnetic data analysis, Geophysics, **63**, 405–410.

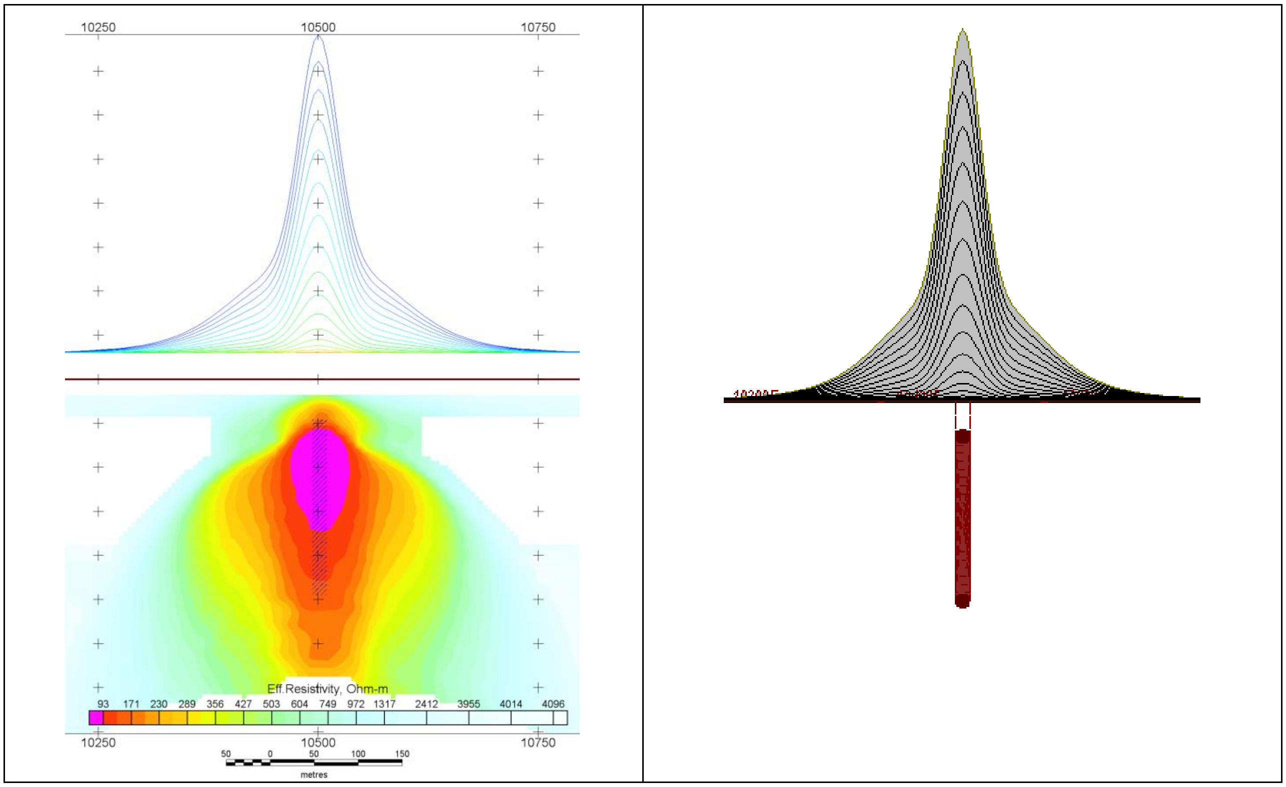


Figure F-2: Maxwell plate model and RDI from the calculated response for "thick" plate 18 m thickness, depth 50 m, depth extend 200 m).

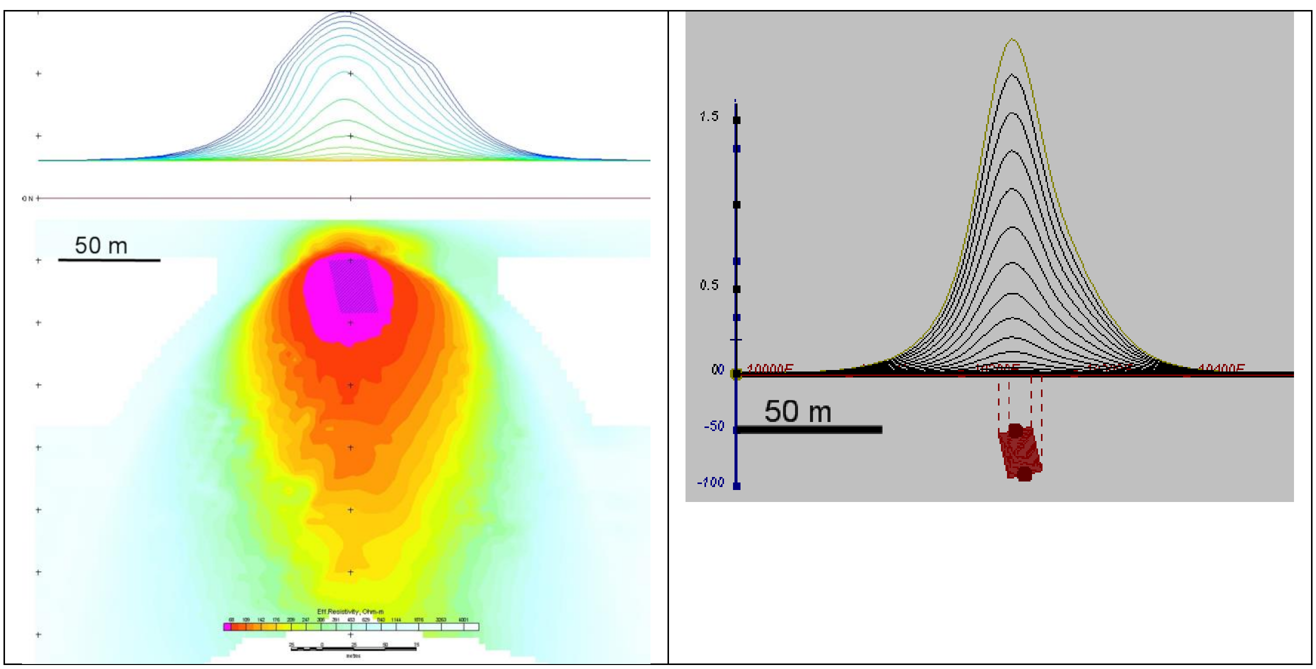


Figure F-3: Maxwell plate model and RDI from the calculated response  for bulk ("thick") 100 m length, 40 m depth extend, 30 m thickness

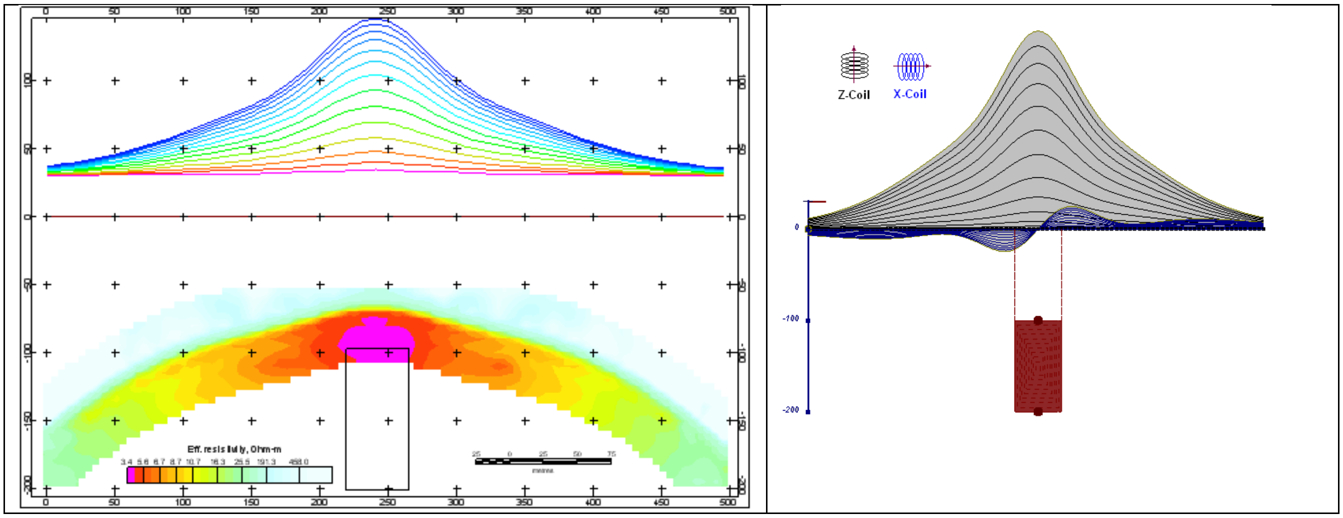


Figure F-4: Maxwell plate model and RDI from the calculated response for "thick" vertical target (depth 100 m, depth extend 100 m). 19-44 chan.

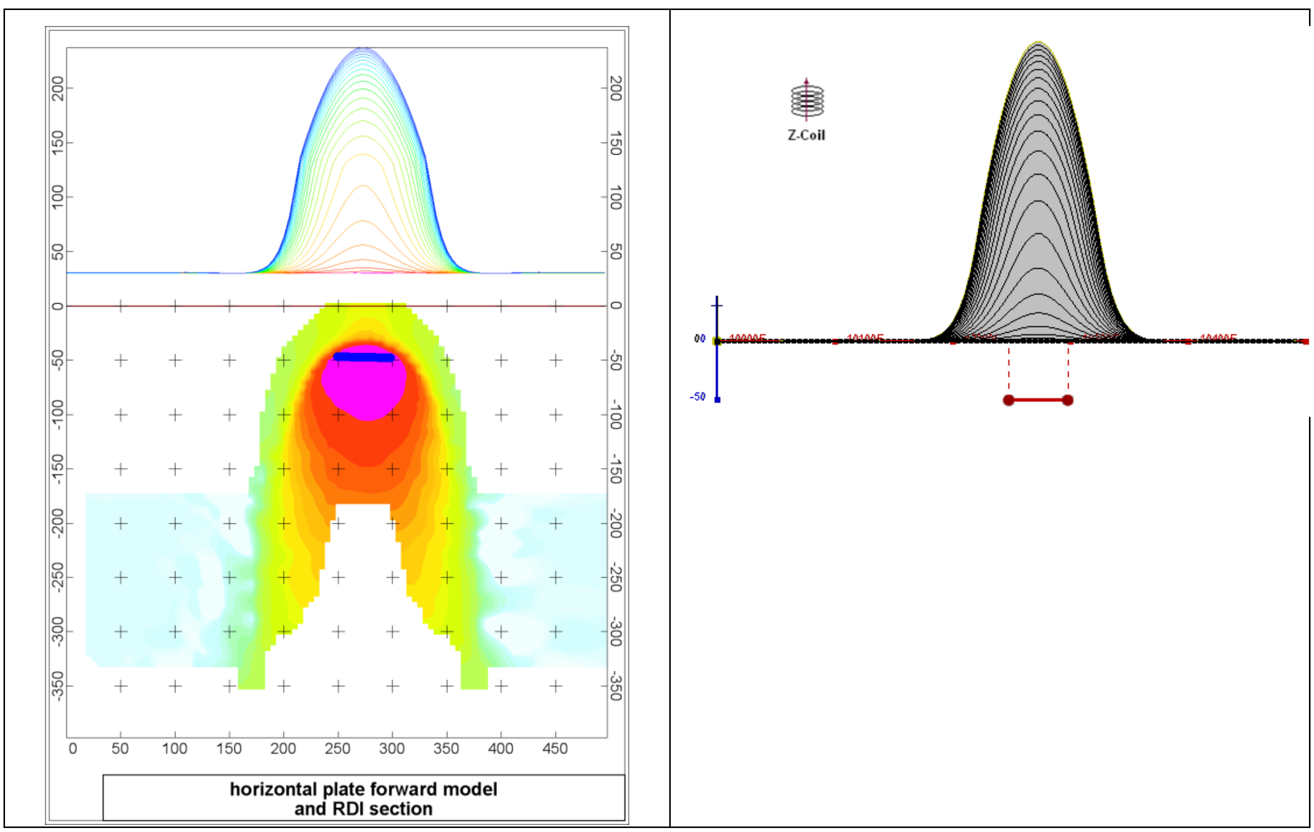


Figure F-5: Maxwell plate model and RDI from the calculated response for horizontal thin plate (depth 50 m, dim 50x100 m). 15-44 chan.

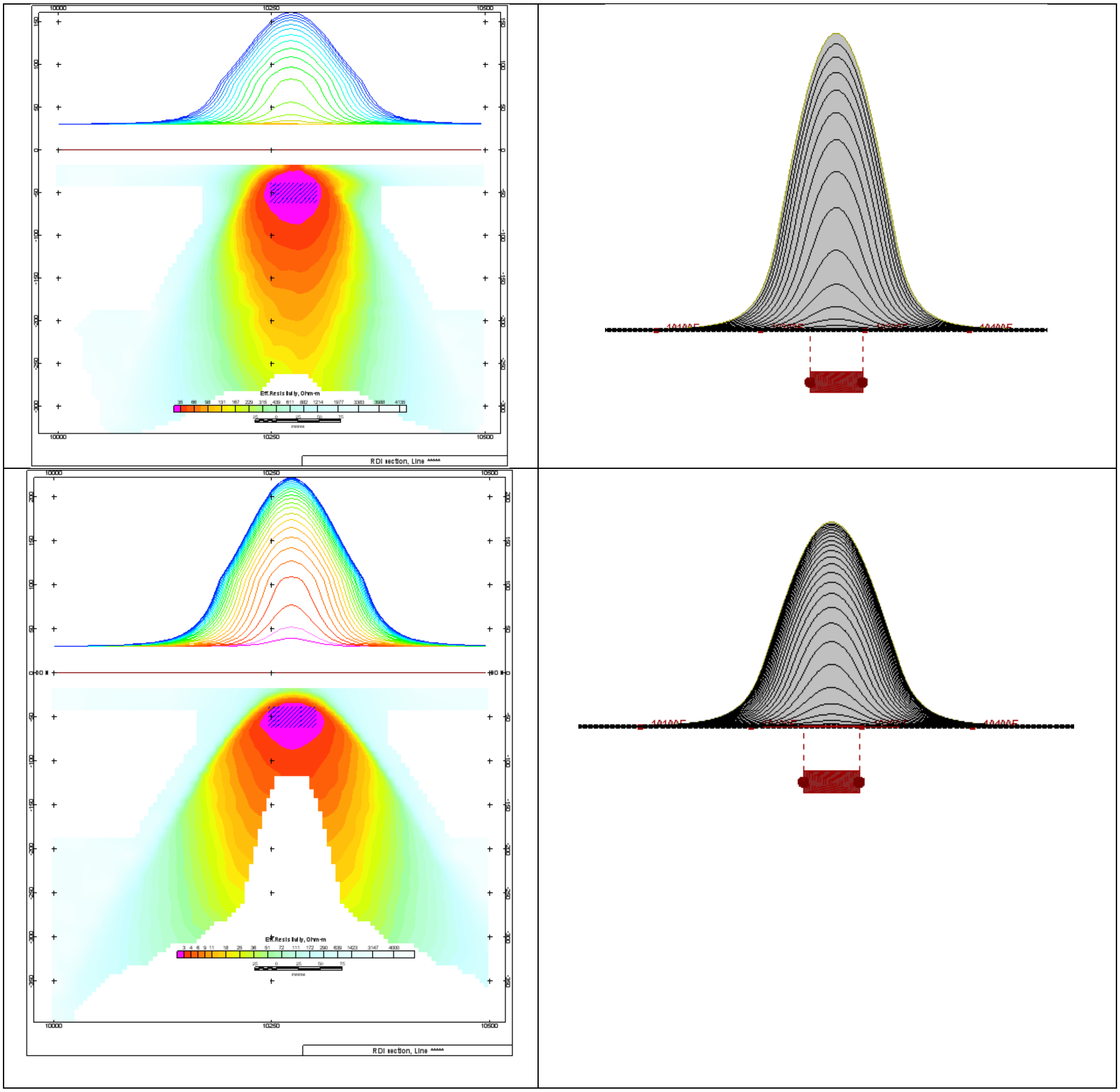

Figure F-6: Maxwell plate model and RDI from the calculated response for horizontal thick (20m) plate – less conductive (on the top), more conductive (below).

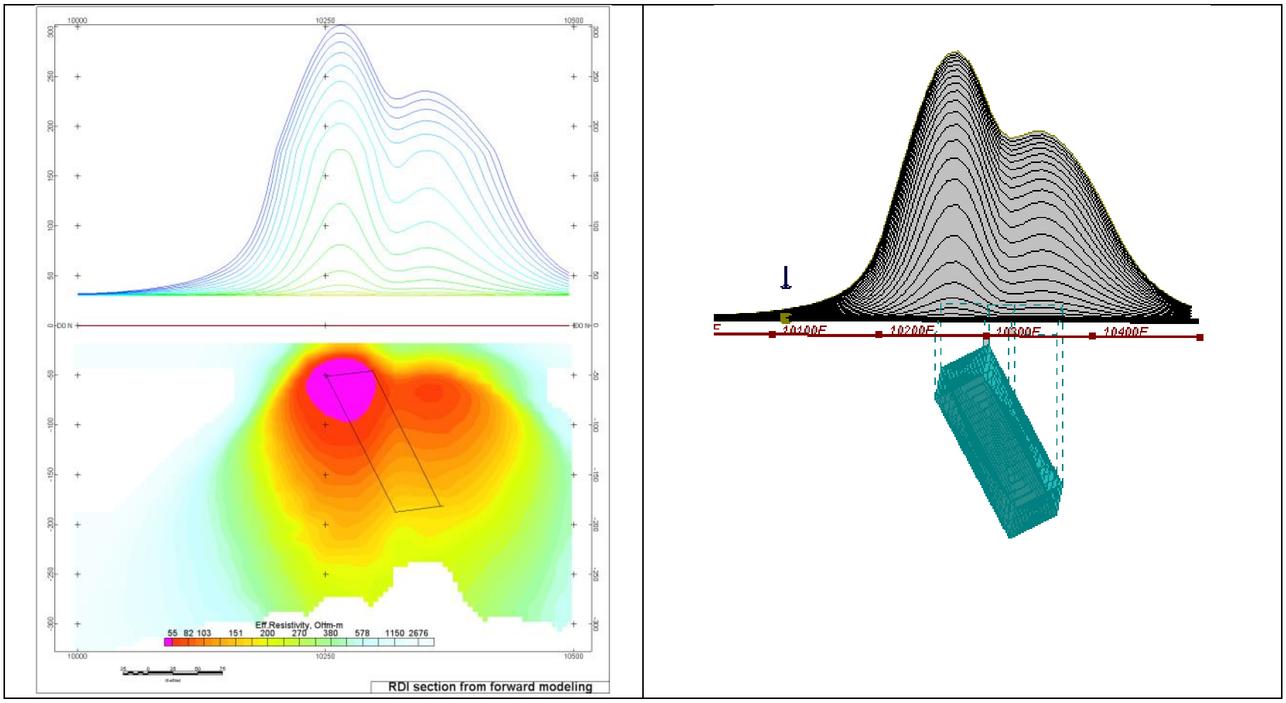


Figure F-7: Maxwell plate model and RDI from the calculated response for inclined thick (50m) plate. Depth extends 150 m, depth to the target 50 m.

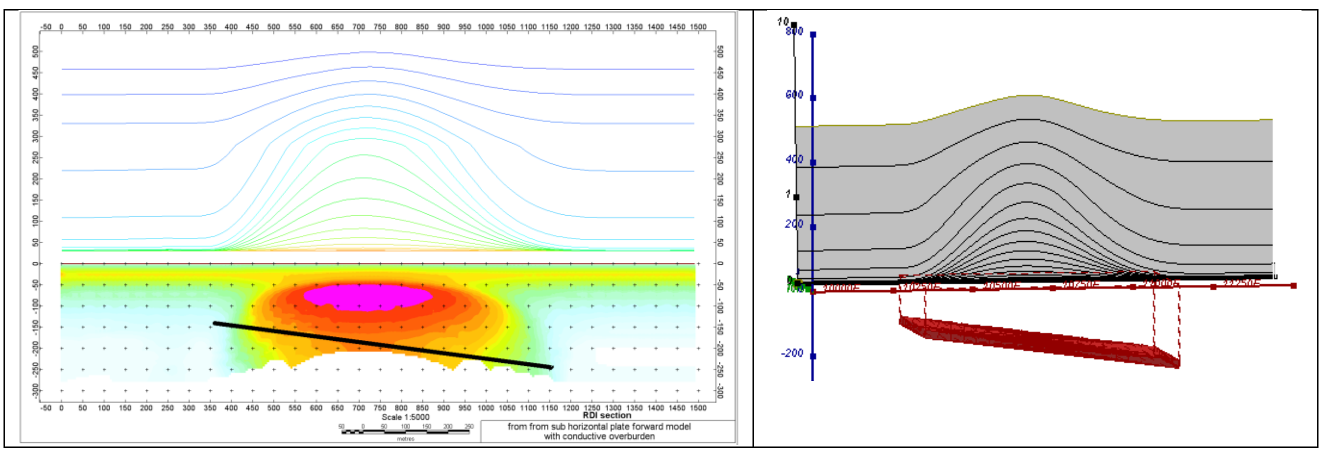


Figure F-8: Maxwell plate model and RDI from the calculated response for the long, wide and deep subhorizontal plate (depth 140 m, dim 25x500x800 m) with conductive overburden.

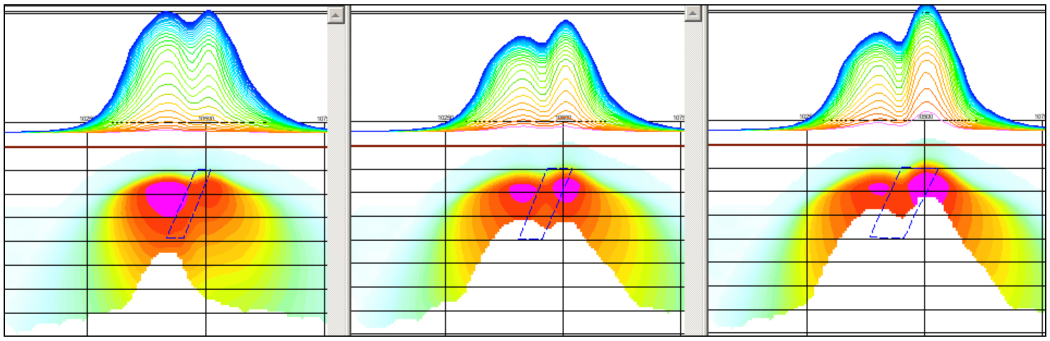

Figure F-9: Maxwell plate models and RDIs from the calculated response for “thick” dipping plates (35, 50, 75 m thickness), depth 50 m, conductivity 2.5 S/m.

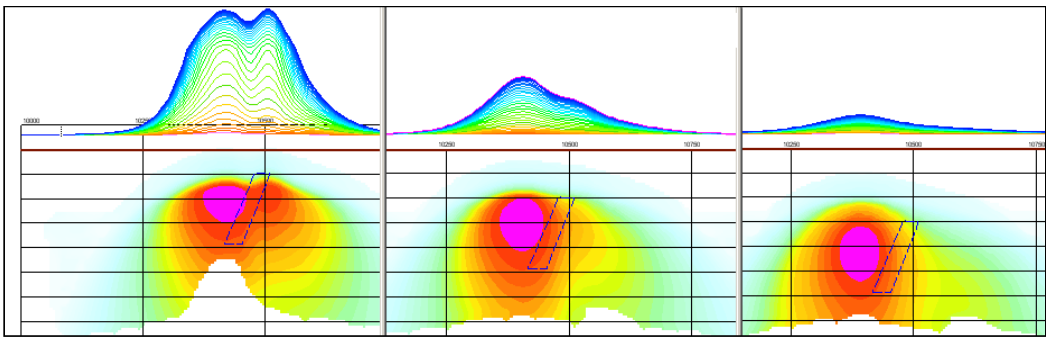

Figure F-10: Maxwell plate models and RDIs from the calculated response for “thick” (35 m thickness) dipping plate on different depth (50, 100, 150 m), conductivity 2.5 S/m.

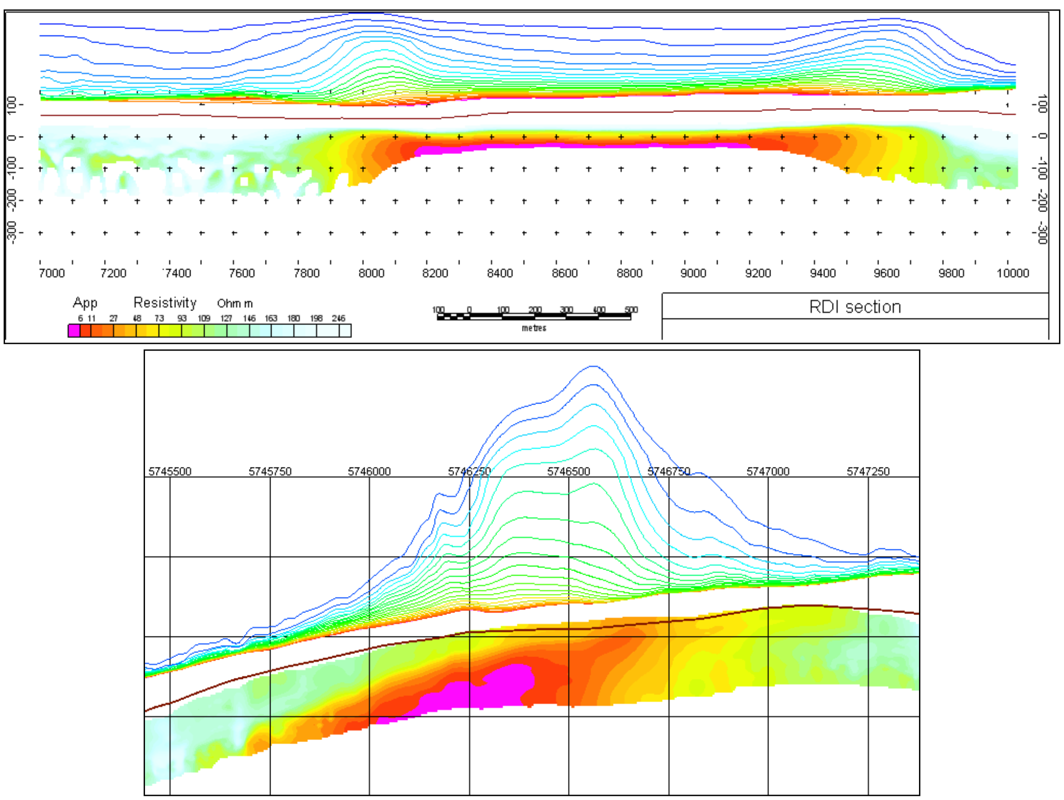


Figure F-11: RDI section for the real horizontal and slightly dipping conductive layers